

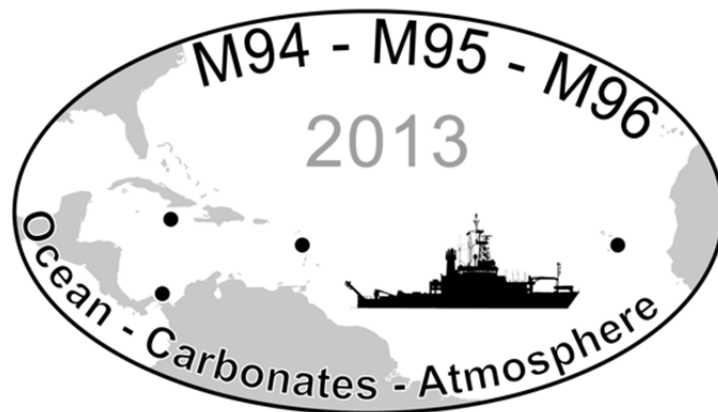
METEOR-Berichte

Ocean - Carbonates - Atmosphere

Cruise No. M96

April 28 – May 22, 2013

Pointe-a-Pitre (Guadeloupe) – Mindelo (Cape Verde)



J. Karstensen

Editorial Assistance:

DFG-Senatskommission für Ozeanographie
MARUM – Zentrum für Marine Umweltwissenschaften der Universität Bremen

2014

The METEOR-Berichte are published at irregular intervals. They are working papers for people who are occupied with the respective expedition and are intended as reports for the funding institutions. The opinions expressed in the METEOR-Berichte are only those of the authors.

The METEOR expeditions are funded by the *Deutsche Forschungsgemeinschaft (DFG)* and the *Bundesministerium für Bildung und Forschung (BMBF)*.

Editor:

DFG-Senatskommission für Ozeanographie
c/o MARUM – Zentrum für Marine Umweltwissenschaften
Universität Bremen
Leobener Strasse
28359 Bremen

Author:

Dr. Johannes Karstensen	Telefon:+49 431 600 4156
Physikalische Ozeanographie,	Telefax:+49 431 600 4102
Helmholtz Zentrum für	e-mail: jkarstensen@geomar.de
Ozeanforschung Kiel	
Düsterbroker Weg 20	
24105 Kiel	

Citation: J. Karstensen (2014) Ocean – Carbonates – Atmosphere - Cruise No. M96 – April 28 – May 22, 2013 – Pointe-à-Pitre (Guadeloupe) – Mindelo (Cape Verde). METEOR-Berichte, M96, 59 pp., DFG-Senatskommission für Ozeanographie, DOI:10.2312/cr_m96

ISSN 2195-8475

Table of Contents	Page
1 Summary	3
2 Participants	4
3 Research Program	5
4 Narrative of the Cruise	5
5 Preliminary Results	8
5.1 CTD measurements and calibration	8
5.2 Vessel mounted ADCP velocity observations	16
5.3 Lowered ADCP velocity observations	17
5.4 Thermosalinograph Measurements of near surface hydrography	19
5.5 Mooring Operations	21
5.6 Biogeographical distribution and activity of diazotrophs	25
5.7 Calipso Satellite Surveys	27
5.8 The FUB Sun and Sky Photometers for Aerosol Remote Sensing	32
5.9 Aerosol, Cloud and radiation measurements: OCEANET	39
5.10 R/V Meteor and Land based observatories: The Barbados ‘match’	41
5.11 Microtops Aerosol and Water vapour survey	44
5.12 Particulate matter (>60 μ m) sizing and imaging with the UVP5	47
6 Ship’s Meteorological Station	52
7 Station list	53
8 Data and Sample Storage and Availability	57
9 Acknowledgements	58
10 References	58

1 Summary

The scientific program of the R/V METEOR M96 expedition was devoted to a combination of atmospheric and oceanic observations. The survey route was oriented along a zonal section from the western to the eastern tropical Atlantic, nominally along 14.5 °N, while the section was started at 11°N (off Trinidad/Tobago).

The atmospheric program addressed primarily processes related to aerosol transport, in particular the impact of Saharan dust. The long-range transport of dust from Africa to North and South America is an aerosol transport with far reaching consequences and with a strong impact on atmospheric processes, such as cloud formation and radiation balance in the tropical Atlantic. In particular the alteration of the aerosols during their westward transport is not well understood and was investigated during M96 with different methods.

The oceanographic program was dedicated to estimating the meridional transport of mass, heat and freshwater in the tropical North Atlantic across 14.5°N. Moreover, the service of the three moorings at 16°N (the MOVE array, operational since 2000) was done. High-resolution hydrography (upper 250m; underway CTD) and currents (upper 1000m; ADCP 38kHz, 75kHz) were recorded and will enable mixed layer and air/sea interaction studies. The biological/biogeochemical program comprised incubation experiments, large volume in-situ pump systems, and underwater video profiling.

Zusammenfassung

Das wissenschaftliche Programm der Reise R/V METEOR M96 hatte sowohl atmosphärische wie ozeanische Zielsetzungen. Die Reiseroute war hauptsächlich entlang eines Zonalschnittes bei 14.5°N, der jedoch bei 11°N (vor der Küste von Trinidad/Tobago) begann.

Das atmosphärische Messprogramm war darauf zugeschnitten, Fragestellungen zu beantworten, die sich auf den Einfluss von Aerosolen (insbesondere dem Sahara-Staub) auf Prozesse in der Atmosphäre beziehen. Der Transport von Sahara-Staub über den Atlantik hinweg in die Karibik und anderswo hat weitreichende Konsequenzen für viele atmosphärische Prozesse, etwa Wolkenbildung und Strahlungsbilanz seien hier genannt. Insbesondere die Änderungen der Aerosole auf ihrem Weg nach Westen sollte, basierend auf den M96-Daten, besser verstanden werden. Dazu wurden unterschiedliche Messverfahren angewandt.

Die ozeanografischen Arbeiten befassten sich mit Messungen zu meridionalen Transporten und mit der zonalen Verteilung von Wassermassen. Dabei ging es im Kern darum, den Zonalschnitt bei 14.5°N detailliert zu beproben. Zudem wurden Verankerungen (MOVE arrays) getauscht, die quasi kontinuierlich den Meridionaltransport auf 16°N erfassen. Es wurde auf dem Zonalschnitt neben konventionellen CTD-Stationen auch eine Unterwegs-CTD eingesetzt, mit der die oberen 250m der Wassersäule mit etwa 10km Horizontalauflösung bei fahrendem Schiff vermessen wurden. Zugehörige Geschwindigkeiten wurden mit den Schiffs-ADCP vermessen. Wasserproben an ausgewählten Stationen wurden für Inkubationsexperimente verwendet. Des Weiteren wurden Filtrationen von großvolumigen Proben durchgeführt, die mit Hilfe von In-situ-Pumpen gewonnen wurden.

2 Participants

	Name	Task	Institution
1	Dr. Johannes Karstensen	Chief scientist	GEOMAR
2	Michael Schlundt	TSG & rain gauge, CTD/uCTD watch	GEOMAR
3	Wiebke Martens	Technician	GEOMAR
4	Dr. Alice Pitrie	uCTD processing, CTD/uCTD watch	GEOMAR
5	Dr. Pieter Vandromme	UVP processing, CTD/uCTD watch	GEOMAR/Excellence Cluster
6	Dr. Taavi Liblik	Salinometer/ADCP processing, CTD/uCTD watch	GEOMAR
7	Till Baumann	LADCP processing, CTD/uCTD watch	CAU
8	Wilma Huneke	Oxygen titration	CAU
9	Christian Begler	Mooring / CTD/uCTD watch	UCSD
10	Dr. Matthias Lankhorst	Mooring / CTD/uCTD watch	UCSD
11	Dr. Sung Hyun Nam	Mooring / CTD/uCTD watch	UCSD
12	Anastasia Boisgard	Mooring / CTD/uCTD watch	UCSD
13	Dr. Ronny Engelmann	OceanNet	TROPOS
14	Alexandra Pietsch	OceanNet	TROPOS
15	Annett Skupin	OceanNet	TROPOS
16	Dr. Stefan Kinne	MicroTops	MPI-M
17	Dr. Gaby Rädcl	Cloud statistics	MPI-M
18	Dr. Thomas Ruhtz	FUBISS-ASA2/AMSSP/MicroTops	WeW
19	Jonas v. Bismarck	FUBISS-ASA2/AMSSP/MicroTops	WeW
20	Sören Testorp	Radiometer/Polarimeter URMS/AMSSP	WeW
21	Dr. Julien Dekaezemacker	Inkubation, Nitrate cycle, in-situ pump	MPI-MM
22	Dr. Wiebke Mohr	Inkubation, Nitrate cycle, in-situ pump	Harvard/ MPI-MM
23	Clara Martinez Peres	Inkubation, Nitrate cycle, in-situ pump	MPI-MM
24	Laura Piepgras	Inkubation, Nitrate cycle, in-situ pump	MPI-MM
25	Martin Stelzer	Meteorology	DWD

GEOMAR: Helmholtz-Zentrum für Meeresforschung, Kiel

CAU: Christian-Alberts-Universität zu Kiel

UCSD: Scripps Institut für Ozeanographie

TROPOS: Leibniz-Institut für Troposphärenforschung

MPI-M: Max-Planck-Institut für Meteorologie, Hamburg

MPI-MM: Max-Planck-Institut für Marine Mikrobiologie, Bremen

WeW: Institut für Weltraumwissenschaften, Freie Universität Berlin

Harvard: Harvard University, Cambridge

3 Research Program

The scientific program during M96 serves several atmospheric as well as oceanographic key questions. The **atmospheric key questions** include:

- How does the composition and density of the aerosol load changes during the zonal transport over the tropical Atlantic?
- What are the local (regional) density, distribution, type, and size spectrum of the aerosol?
- Is there a connection between aerosol load and cloud formation? Is there a feedback of the cloud formation on the aerosol load/composition (e.g. size)?
- Quantification of the local/regional radiation balance and what is the impact of the aerosol load and clouds?

The **oceanographic key questions** to be addressed during M96 include:

- Determine the hydrographic and biogeochemical distribution along 14.5°N and compare those with a survey along that section from 1989. Are there systematic changes? And can these changes be related to other oceanic or atmospheric changes?
- Quantify the integrated mass, heat and freshwater transport across 14.5°N.
- How do the synoptic section compare to the end point geostrophic array along 16°N (MOVE)? Determine the depth and characteristic of the near surface (upper 150m) hydrography. Is there a link to the atmospheric radiation balance?
- Can differences between the western and eastern tropical North Atlantic particles be identified?
- Are there zonal gradients in the upper layer nitrogen cycling?

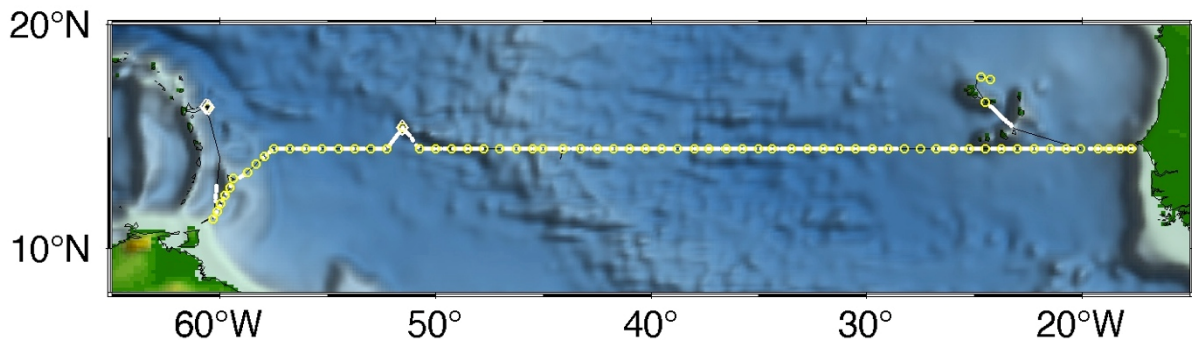


Fig. 3.1 Track chart of R/V METEOR Cruise M96 projected on a bathymetry from Smith and Sandwell (1997). CTD (yellow circles), mooring positions (rhombus), and uCTD stations (white dots) are given along the cruise track (black line). Note the last 4 Stations off Senegal have been surveyed during R/V METEOR Cruise M97 (Chiefscientist: Dr. Toste Tanhua, GEOMAR, Kiel, Germany).

4 Narrative of the Cruise

By 26 April representatives of the teams from GEOMAR, Scripps Institution for Oceanography (SIO), TROPOS, MPI-M, MPI-MM and WeW arrived in Pointe-a-Pitre to set up the equipment

on R/V METEOR. Unfortunately a box tower that contained the two CTD control units (GPS receiver, SBE11, industry PC and monitor) as well as some spare parts was seriously damaged during the loading from the pier to the ship and replacements had to be organized. The OCEANET container with the Raman-lidar was set up on the port foredeck, the spectral radiometer were set up on the upper deck and other Meteorological sensors as well. On Saturday morning a computer shop was visited and replacement parts bought to repair at least one of the CTD control units PCs (which both did not work after the damage). At least based on our tests, both SBE11 were still operating so were the GPS receiver. The rest of the Saturday was used for further installations of the equipment. In particular the mooring operations were prepared, which were scheduled already a few hours after leaving port, but all other systems as well.

On Sunday, 28 April between 08:00 and 08:30 (all times are in local time) the ship was screened for stowaways. We left the pier at 08:36 and started the M96 expedition. At 12:08 (16°11.0'N/60°59.8'W) the underway system (TSG, Meteorology, ADCP 38 kHz, 75 kHz) were started and the scientific program begun. At 14:41 the release command was sent to the M4 mooring which was on deck at about 18:45. The rest of the night was used for two CTD casts (1000m, 3500m) which were also used to calibrate MicroCats (4 times 8 minutes stop) foreseen for the deployment of M4 and M3 as well as to test the Benthos release systems. The first cast had to be repeated a few times, exchanging the SBE11 deck unit, the winch, and the cable connection between the rosette sampler and the CTD. On Monday (29.4.) morning at 05:30 the release command was sent to the M3 mooring. However, it took approximately 4h to locate the mooring most likely because it went adrift after deployment as well as after release. At 14:47 the mooring was completely recovered. Deployment of the mooring was prepared but postponed to the next day. Instead an attempt was started to acoustically retrieve data from a PIES – but this attempt failed, no data was received. A 4 hours in-situ pump cast was also done with two pumps, while one of the pumps failed. At 05:42 the deployment of the 4900m long M3 mooring started by releasing the head buoy to the water about 10.5nm away from the nominal position. M. Lankhorst (SIO) chose the distance. After releasing all gear to the water we still had about 3 hours of steaming to reach the target position (0.6nm over the targeted mooring position). In the afternoon, we also deployed M4 (again we had to tow the mooring behind the ship for more than 2 hours to reach the launch position). R/V METEOR then left the working area off Guadeloupe and moved south, toward the coast of Trinidad/Tobago to start the core operations along the zonal section crossing the Atlantic. On 1 May we installed the W1 (University of Hamburg) Oceanscience underway CTD system (uCTD) on the aft of the portside of R/V METEOR. Two systems (uctdW1, University of Hamburg; W2 GEOMAR) were on board. After a first trial with a dummy probe the real probe (#67) was used. Moreover the tanks for the incubation experiments were erected on the main deck and the Underwater Video Profiler (UVP) was installed on the CTD rosette. Unfortunately the UVP had to be mounted outside the frame in a special attachment, which leads to a tilt of the rosette system. According to the IADCP analysis the angle was not critical. Around 19:00 an uCTD probe (#67) was lost. The winch system did not reveal the wire quick enough and the probe came unexpectedly quick (after a few 10 seconds) back to the ship and stucked on the block, was detached and fell into the Atlantic.

At 22:20 we began to survey the zonal section across the Atlantic at nominal 14.5°N. The CTD work was accompanied by uCTDs, but now using the uctdW2 (GEOMAR winch system), which spooled much smoother than the uctdW1. First we are heading northeast, on the eastern

side of Barbados, towards 14°30'N which is then followed across the Atlantic, except of a short de-turn to recover the M1 mooring at about 16°N. In the evening M. Lankhorst presented the MOVE array to interested scientists during our daily scientific and logistics meeting. On Thursday, 02 May we continued our north-eastern course with CTD profiles and uCTDs in-between (at full ship speed ~11kn). In the late afternoon, close to Barbados, an atmospheric data survey, in conjunction with a land-based observatory operated by the MPI-M, was conducted. During the „19:00 meeting“ S. Kinne gave an overview talk about the Barbados observatory (title: “Why Barbados?”). On Friday, 3 May the CTD/uCTD program continued.

A first dust event (according to the polarization observed with the Lidar) was detected, that fitted well to the prognostic/forecast models. Another MicoCat calibration /releaser test cast (5500m) was done for the instrument preparation for the upcoming M1 deployment. Mostly full depth/3000m profiling was done. At some stations for scientific reasons a number of consecutive deep casts were profiled. On Saturday, 4 May the CTD/uCTD program continued. Risk assessments for the operation of the uCTD and the OCEANET container were prepared for the ship. Two calibration casts (1000m, 3500m) were done. It was discovered that virtually all screws of the uCTD system had to be carefully observed and tightened regularly. The clutch of the W1 uCTD winch was cleaned. On Sunday the sampling with the uCTD was changed from as fast as possible (we always used the rewinder!) to every 30 minutes. Regular atmospheric and ocean program continued. On Monday, 6 May, the recovery of the M1 mooring (10th) begun at 06:00 and was complete during the morning. A PIES was deployed and the deployment of the M1 mooring (11th) was done in the afternoon. A CTD cast and a 4h pump station were also done. Then we steamed back to the 14.5°N section by doing uCTD. In the morning of 7 May we passed by the NTAS buoy (photographs were taken). Reducing the uCTD sampling to every 0.5 hours cooled the winch down. On May 8th the CTD program was started again, while in the night a satellite (CALIPSO)/ship based (OCEANET) lidar intercalibration experiment was conducted. The intersection points and times along 14.5 N revealed an overpass of the Calipso satellite in the early morning and the Meteor was directed to follow the path over a period of 5 hours. During the survey, the OCEANET lidar detected some polarized particles (but not much Saharan dust). The following days the standard program along the section was continued: CTD, uCTD, IADCP, atmospheric measurements. P. Vandromme presented the UVP observations in the daily 19:00 meeting. On Sunday, 12 May we expected water depth deeper than 6000m and the winch was changed to W10. Moreover, the CTD was mounted to the spare rosette and UVP, backscatter, and altimeter were unmounted as they are only pressure resistant to 6000m. The approximate depth for the cruise planning were extracted from the ETOPO2 data set – but it was found that the data set was particularly unreliable for the deeper depth, which may be related to some spline interpolation of sparse deep soundings. As such, most casts were less deep than expected and the deepest cast, expected to be 6800m was only 6300m. The CTD was mounted back to the other rosette and all sensors were added again (as we did not expect depth > 6000m). On Tuesday 19:00 Jonas v. Bismarck gave a talk. On Wednesday, 15 May a problem with the IADCP control unit was found (connector corrupt) and we changed to the spare one. We also had to change the upward looking IADCP instrument. On Thursday, 6 May Ronny Engelmann give a short presentation on the OCEANET container observations and instrumentation and Stefan Kinne on the “A-train” satellite group. We changed in the night the W2 winch of the uCTD system back to the (cleaned) W1 and oiled the W2 chain.

We entered into the EEZ of the Cape Verdes. Many clouds hinder the atmospheric measurements. On Friday, 17 May the deckbox #1 of the IADCP was exchanged by #2 as problems occurred. We also started to cool down the uCTD sonde with surface water before launch, as there seem to be a temperature effect on the first meters measurements. On 18 May we changed the W1 back to W2 as W1 was still (also cleaned clutch) too slow spooling. That evening, the dinner was served as a Barbecue on deck. On Monday the 20th May the 14.5°N section was completed at the border to the Senegalese EEZ (020°W). We turned northwest and steamed towards the southern Cape Verde Island (Maio) to start auCTD section through the archipelago (9 knots steaming and 500m depth coverage). The uCTD section started on Tuesday at 06:00. In the afternoon, at 17:00 a UVP yoyo cast during the sunset was performed to study the vertical migration of zooplankton. Then we headed towards a 2nd Calipso satellite track intercomparison survey. The survey was done on Wednesday 00:00 -03:00 and after finalizing, we steamed toward the Cape Verde Ocean Observatory (time series), north of the Island Sao Vicente. We stopped on our way at 04:00 to do another UVP/ yoyo cast, this time to resolve the vertical migration during sunrise. A last CTD cast was done at the CVOO site and then we steamed towards Mindelo, arriving at 18:00 in the harbour. Registration of scientific data stopped at 15:00. In the morning of the 23th May the unloading of the containers begun.

5 Preliminary Results

5.1 CTD measurements and calibration

(Taavi Liblik, Wiebke Martens, Johannes Karstensen)

During RV Meteor M96 a total of 67 CTD stations were acquired. Except of profile 41 to 45, which were expected to reach deeper than 6000m, the rosette #1 was used. The rosette #1 configuration included a SBE 9 plus CTD – System (GEOMAR #SBE3) with an altimeter and a Wetlabs Fluorometer. The rosette contained 21 Niskin bottles of 10l each. Moreover, an „Underwater Video Profiler” (UVP; see respective chapter) and two 300kHz up/downward looking IADCP - System (see respective chapter) were installed. For profile 41-45 the rosette #2 (GEOMAR) was used and, as instrumentation was not adequately pressure tested, only the CTD and the bottles were used. For these casts the depth was retrieved from the ships echo sounder only (no altimeter verification).

The SBE#3 was equipped with double sensor packages for temperature, conductivity and oxygen. The temperature and oxygen sensors were serviced and calibrated just before the cruise in February and March 2013 at the manufacturer Seabird. Adding 5 eastern most stations from RV Meteor M97 a complete zonal sections of hydrography and oxygen, along nominal 14°30'N, was recorded (Fig. 5.1).

Mooring instrumentation for deployment and after recovery was attached to the rosette and CTD-profiles were used later for calibration.

CTD-conductivity calibration

The GEOMAR Guildline Autosalsalinometer #7 (Model 8400 B, operated by T. Liblik) was used for calibration of the primary and secondary conductivity sensor. Calibration measurements

were typically performed around 16:00-20:00 local time. Calibration of the salinometer was done in reference to the IAPSO Standard Seawater (P154, $k_{15}=0.99990$). In addition, two sub-standards (25 litres of seawater of unknown but constant salinity) were used to trace the stability of the salinometer. On 15 May a small air bubble was found in the upper part of the rightmost cell tube. We tried to remove it by rinsing the system with mucosal solution but it didn't help. However, since the bubble was well above the measurement spiral, it didn't impact the measurement quality. This could be confirmed by re-standardization and routine measurements of the Sub-standard water. A drift could not be detected from the substandard measurements during the analysis period (see Fig. 5.1.).

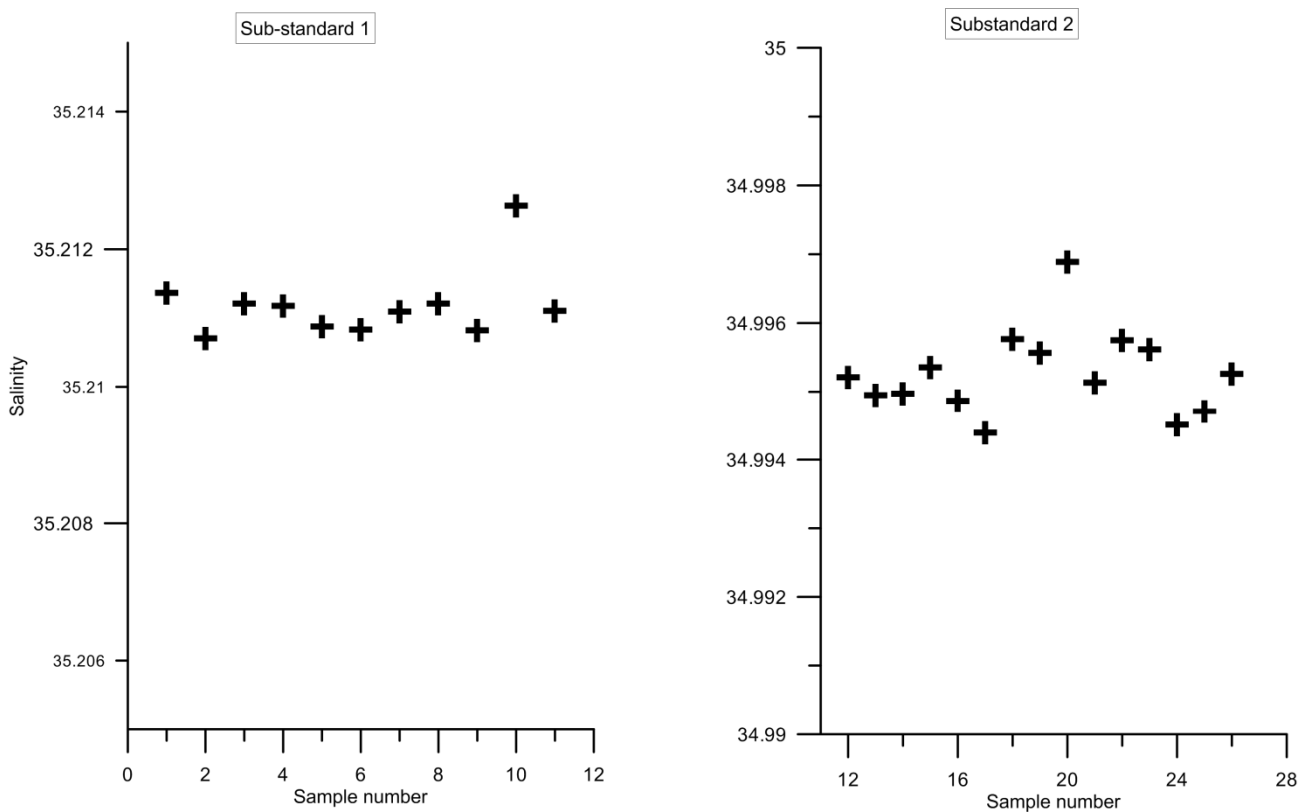


Fig. 5.1 Evolution of the substandard measurements (two different batches were used) in relation to sample number.

Overall 209 calibration points from the Salinometer measurements were obtained for the calibration. To account for possible outliers in the salinometer data, 33% of the largest differences between CTD and bottle samples were discharged and not considered for calibration. The projection from the bottle stop of the up- to the downcast was done by searching for similar potential temperatures within 30dbar pressure interval around similar pressure horizons between up- and downcast. For the critical loop edit velocity 0.01 m/s were used. The conductivity calibration of the downcast data was performed using a 1st order linear fit with respect to temperature, pressure and conductivity (Table 5.1).

CTD system SBE#3 (profile 1 to 67)		
P calibration or check date :	2010/8/17	
Pressure Deck offset applied to data	1.125000	
Sensor pair used for calibration	1	
Pressure S/N	82991	
Temperature S/N	4835	2120
Conductivity S/N	3374	3300
Oxygen S/N	1287	1718
Calibration results system #1 (used for final data)		
C down calibration string:	-0.0012896-3.0685e-08*p-5.7134e-05*t+0.0004819*c	
misfit	0.0009 PSU	
O down calibration string :	2.3532+0.0018549*p-0.17712*t+0.055361*o	
misfit:	0.95 $\mu\text{mol/kg}$	
C up calibration string:	0.0025639+1.9324e-08*p+6.9097e-05*t-0.00085628*c	
misfit:	0.0007 PSU	
O up calibration string:	0.23295+0.0017728*p-0.15446*t+0.064659*o	
misfit:	0.95 $\mu\text{mol/kg}$	
Calibration results System #2 (not used for calibration)		
C down calibration string:	-0.00056476-3.5481e-08*p-1.5922e-05*t+0.00027867*c	
misfit	0.0012 PSU	
O down calibration string:	3.1046+0.0024867*p-0.16562*t+0.063992*o	
misfit:	1.374 $\mu\text{mol/kg}$	
C up calibration string:	-0.0011625-3.2744e-08*p-3.4341e-05*t+0.0004734*c	
misfit:	0.0008 PSU	
O up calibration string:	1.9056+0.0023793*p-0.14852*t+0.071144*o	
misfit:	1.37 $\mu\text{mol/kg}$	

Table 5.1 End of cruise salinity and pressure summary of calibration information for the two CTD systems used during R/V Meteor M96 (as of 01. August 2013, see data archiving for access to the latest version).

Technical problems

Some technical problems occurred during the cruise and are listed below: Sensor cables were replaced (cast 1, 2); the altimeter did not respond and the CTD frame touched the ocean bottom (cast 18), no impact was detected. At station 36 the UVP switched on late, so the profile was restarted.

At the beginning of the cruise some Niskin bottles were blocked and difficult to close/prepare, O-rings were replaced. Due to a defect magnet, bottle 6 did not close (cast 23 & 24) and the SBE32 Carousel Water Sampler was replaced after cast 24. The magnet was replaced later in the lab. The ships power supply failed, so the PC and Deck-Unit broke down and the profile was restarted (cast 7). A UPS was installed to prevent further power outages. During a couple of casts the winch had to stop on the upcast as there were problems with the correct layering of the wire.

Oxygen calibration

A total of 503 discrete water samples were taken from selected depths for oxygen measurements by Winkler titration. Samples were taken with 100 mL WOCE bottles with well-defined volumes from a majority of the CTD rosette casts in order to calibrate the SBE43 oxygen sensors attached to the CTD. It was ensured that the sample bottles were flushed with at least 3 times its volume

and the samples were free of air-bubbles. At most CTD casts, a duplicate from one of the Niskin bottles was taken in order to quantify sampling and titration uncertainties.

Oxygen was determined by Winkler titration within 12 hours after sampling following standard protocols (Langdon, 2010). The precision of our Winkler-titrated oxygen measurements (1σ) was $0.31 \mu\text{mol} \cdot \text{kg}^{-1}$ based on 79 duplicates. By comparing the standard solution with reference materials from WAKO inc. (USA), the standard solution $\text{KH}(\text{IO}_3)_2$ was found to be accurate to better than 0.01 %.

The CTD oxygen downcast for CTD systems is calibrated by using 67% of the joint data pairs between downcast CTD sensor value and titrated oxygen. For the calibration a linear correction polynomial depending on pressure, temperature and the actual oxygen value was fitted. Hence, a total amount 247 data points for CTD system SBE#3 was recorded, which results in an RMS-misfit of order $0.95 \mu\text{mol}/\text{kg}$ for the primary SBE43.

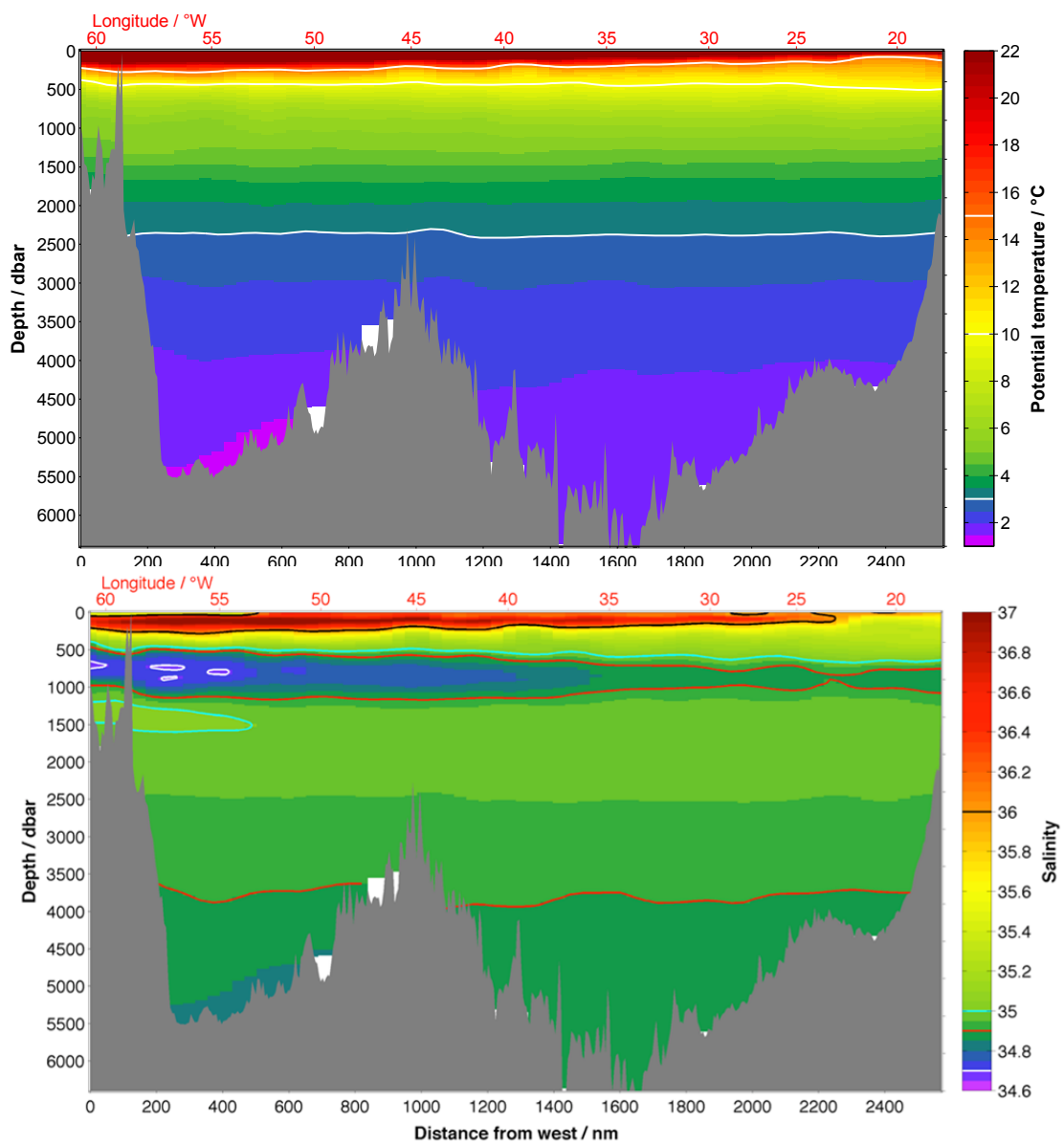


Fig.5.2a Temperature (upper) and salinity (lower) distribution along the zonal section at nominal 14.5°N (includes R/V Meteor M97 data at the eastern boundary) in respect to the distance (km) from the western most station (lower axis label). For reference the longitude in $^\circ\text{W}$ is given on top of the figure

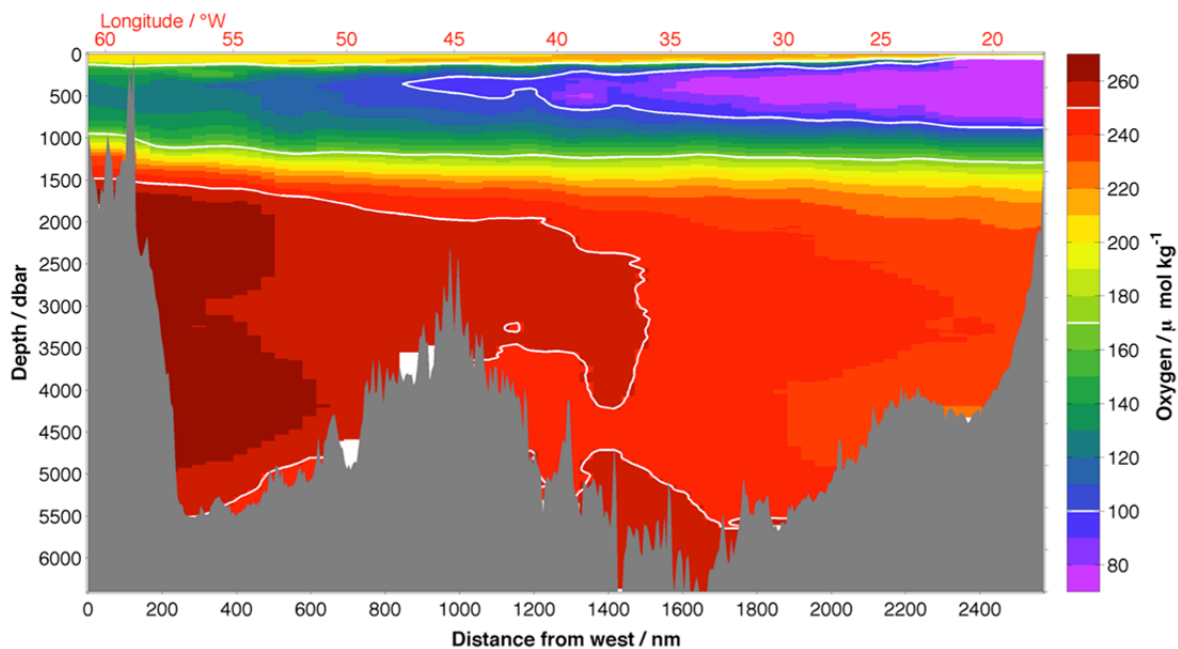


Fig. 5.2b Oxygen distribution along the zonal section at nominal 14.5°N (includes R/V Meteor M97 data at the eastern boundary) in respect to the distance (km) from the western most station (lower axis label). For reference the longitude in °W is given on top of the figure.

The strongest zonal gradients (Figure 5.2a, b) can be seen in salinity and oxygen along the 14.5°N section. Emanating from the western boundary the section through the North Atlantic Deep waters is clearly evident in both sections (higher oxygen and more saline). The northward penetration of Antarctic Bottom water is seen east of the Midatlantic Ridge as well. The Existence of the North Atlantic Oxygen Minimum Zone is visible by the core of low oxygenated waters located at about 500m depth in the eastern part of the section. With a core at about 750m depth, the northward penetration of the Antarctic Intermediate water is seen.

uCTD System

During M96 cruise, data was collected from 30 April to 21 May using an underway CTD (uCTD). This system was used to survey mostly the upper 200 m of the water column in order to observe the variability in the mixed layer and to identify low salinity lenses in the western part of the Atlantic. A total of 349 profiles were recorded with an averaged depth of 250 m (maximum depth was 550m). The measurements were performed from the ship moving at speed of about 11kn. A main section across the Atlantic, along the latitude 14.5°N was realized with an averaged horizontal resolution of ~8 km (Fig. 5.3 & 5.4). Another section through the Cape Verde archipelago (16 profiles) was recorded with 9kn and to 500m depth. A time delay of 30 minutes between each profile was chosen in order to have a fairly constant horizontal resolution and to be able to do maintenance on the device between casts.

The uCTD consists of a probe equipped with temperature, conductivity and pressure sensors from SeaBird, a tail and a winch. The probe records the data with a frequency of 16 Hz. For most of the profile, 250 m of rope were spooled on the tail, and the duration of recording during the

dive was of 100 seconds, which led to 1600 recordings per cast and an averaged vertical resolution of ~ 0.12 db.

Two winches, one used several times in the past (W1) and a brand new one (W2), three probes (#68, #69, #126), and two dummy probes were available. Some technical problems arose during the cruise. After 10 profiles the W1 winch wasn't unwinding freely anymore and W2 was installed. Due to the problem with W1, one probe (#69) was lost. After 300 profiles the W2 winch was removed because of some undefined noises that appeared when spooling the rope back. The cleaned W1 was used again, but the problems with the freely spooling still existed. In the meantime W2 was cleaned and the chain lubricated and W2 was used again without problems until the end of the cruise.

Loose screws were a problem throughout the operations. At one stage the block situated at the end of the davit detached itself during one cast. It was recovered and fixed on the arm again, after that the block fixation was checked regularly. Concerning the probes, it was necessary to check the screws at least every five casts, as they were getting loose. Besides it was very difficult to recover the probe without hitting the boat, even with the help of a pole.

The system was installed on the stern but without a particular sun protection. The probe was heating up between cast and it was recognized that the first samples of the profiles might be influenced by the temperature changes (with corresponding impact on the salinity). This heating seemed to introduce an apparent diurnal cycle in the upper 10m or so of the profiles, and not confirmed by corresponding SBE911 CTD observations. Therefore the probe was cooled down with freshwater before each cast. However, the diurnal cycle remained and as such is considered to be real at this stage. Moreover it implied that SBE911 observations might not resolve the shallow diurnal cycle most likely because of the turbulent mixing introduced by the system when operated with a UVP. In that case the CTD is lowered to first 10 and then 20m and then is coming back to just below the surface from where what is considered the downcast begins.

A preliminary calibration was applied to the salinity data. A lagged temperature time series $T_c = T - (\alpha - \beta dP/dt) * dT/dt$ taking in account the vertical velocity of the dive (dP/dt) was used to compute salinity. Assuming homogeneity in a few staircase structures that have been recorded in the western part of the section, the best correction for the whole mission appears to be $\alpha = 0.09$ s and $\beta = 5 \times 10^{-3}$.

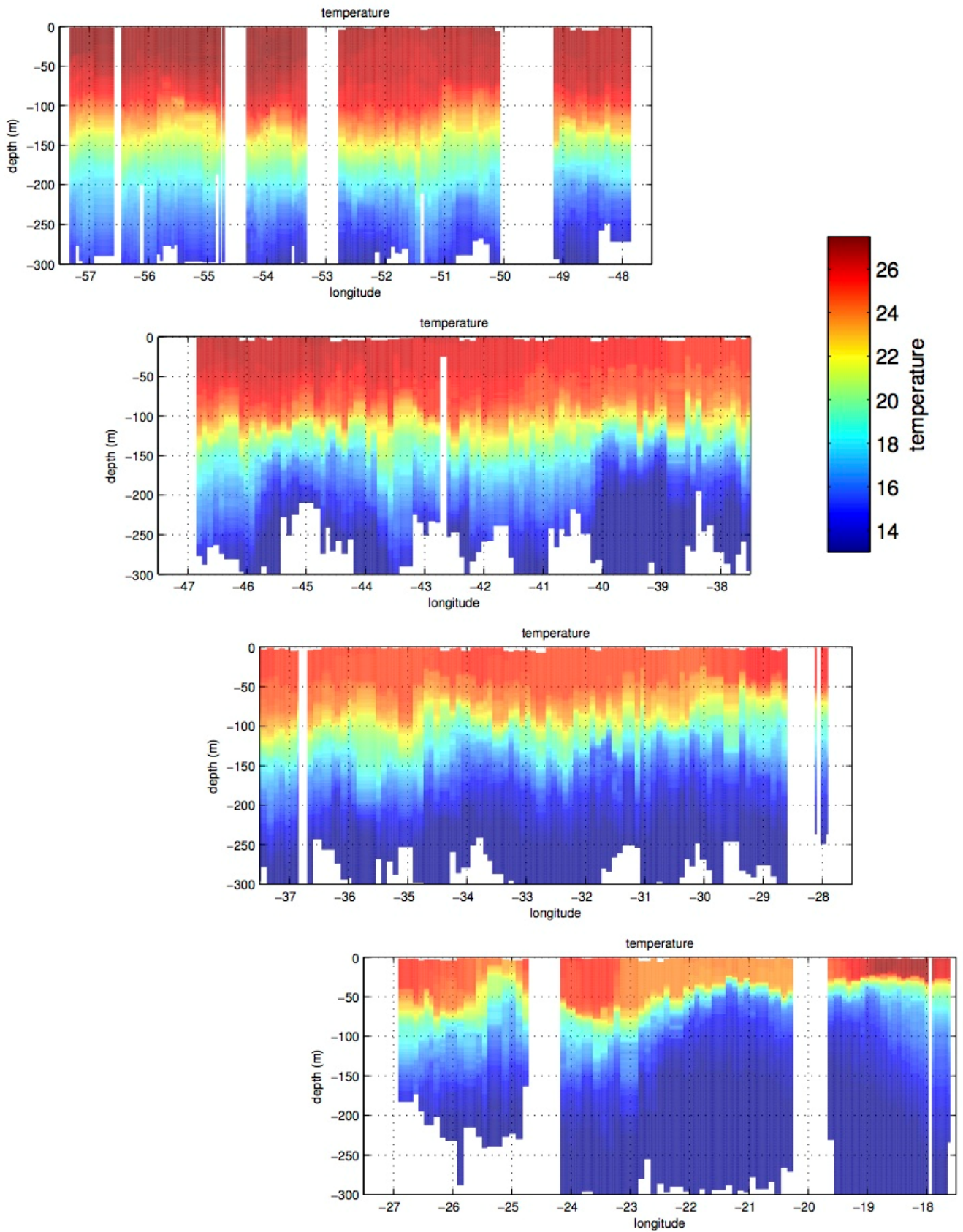


Fig.5.3: Temperature distribution along the zonal section at nominal 14.5°N as obtained from the Underway CTD

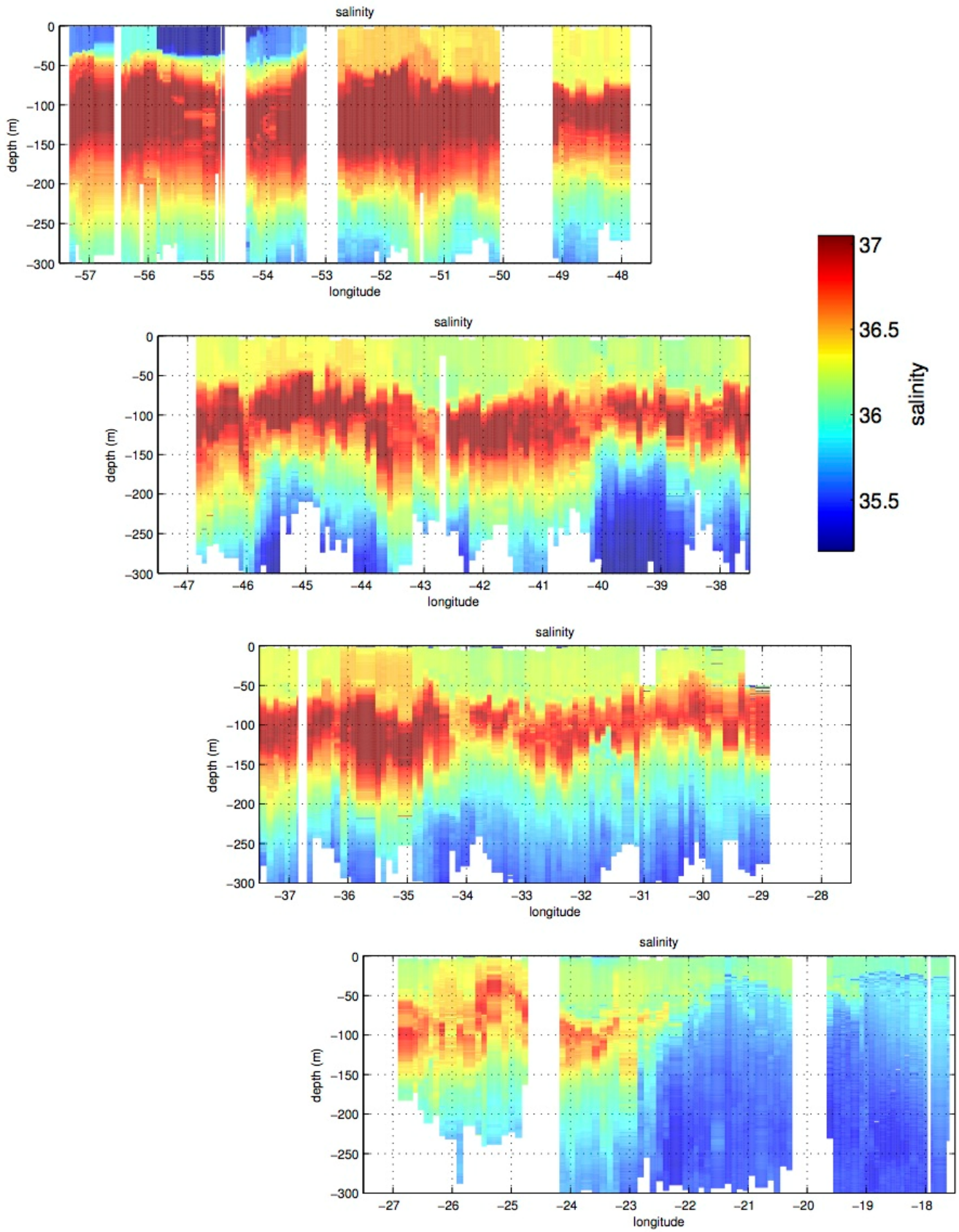


Fig. 5.4 Salinity distribution along the zonal section at nominal 14.5°N as obtained from the Underway CTD

5.2 Vessel mounted ADCP velocity observations (Taavi Liblik)

Current measurements have been performed using the two RDI Ocean Surveyor (OS) instruments (38kHz and 75kHz) of the R/V METEOR. Both instruments were initially configured in broadband mode. Due to noisy signal OS75 we later switched to narrowband mode. We tried to switch back to broadband mode a couple of times, but without success (noise still remained) and therefor decided to stay in narrowband mode.

The OS75 was set up to measure 8m bin size and covered a range of 500 to 700m. The OS38 was configured to use 16m bins and covered a range down to 800 and even 1000m depth, depending on sea state and ship's speed. The OS38 was mounted in the moon pool with approximately zero degree alignment, while the OS75 was mounted at a 45 degree angle to avoid interference between the two instruments. The ADCP acquisition system was recording the ships navigational input. It worked smoothly, except for one occasion on May 15 around 17:00-20:00, where the NMEA data was not available. Moreover, the data recording was interrupted a couple of times due to power outages on the ship, but a UPS device was installed to prevent outages of the system. Both instruments were switched off in Dominica waters (1 May, 01:40 to 04:14 UTC). Information about all interruption events can be found from ADCP log (Table 5.1)

Simultaneous use of the ship's Doppler log and/or echo sounder should be avoided as it degrades the velocity data. The echo sounder was turned on and off only to receive information of water depth at each CTD station. The software VMDAS was used to set the ADCP's operating parameters and to record the data. The Ocean Surveyor data conversion and final data processing was done using GEOMAR vmADCP-Matlab routines last changed by T. Fischer in April 2012.

28.04, 16:08 UTC: ADCP 38KHz was switched ON in broadband (BBM) mode
28.04, 16:13 UTC: ADCP 75KHz was switched ON in broadband mode
29.04, 04:46 UTC: ADCP 38KHz screen was frozen, it was restarted.
29.04, 18:30 UTC: Both ADCPs restarted, due to power outage
29.04, 23:38 UTC: Switched off for acoustic survey
30.04, 10:04 UTC: Bad data quality in depth range 250 - 500 m (75KHz)
30.04, 11:04 UTC: Restarted 75KHz in narrowband (NBM) mode.
01.05, 01:40 UTC: Switched off ADCPs (border crossing)
01.05, 04:14 UTC: Switched on ADCPs
02.05, 18:51 UTC: Power outage, restarted ADCPs
03.05, 14:41 UTC: ADCPs off due to echo sounding
03.05, 15:34 UTC: Power outage, restarted ADCPs
04.05, 12:26 UTC: Switched off ADCPs (problem with PCs)
04.05, 13:03 UTC: Switched on ADCPs
05.05, 00:20 UTC: Switched back to BBM (75 KHz)
07.05, 15:04 UTC: Switched off-on ADCPs, 75 KHz was restarted in NBM
09.05, 23:28 UTC: Both PCs had restarted (unknown reason).
10.05, 11:00-11:30 UTC: Switched off and ON (and as later noticed, 75 KHz was restarted in BBM)
11.05, 12:37 UTC: Switched to NBM (75 KHz)
14.05, 15:35 UTC: ADCPs restarted
15.05, 20:08 UTC: Problem with NMEA, ADCP's restarted

Table 5.2 Summary of ADCP events during R/V METEOR M96.

5.3 Lowered ADCP velocity observations (Till Baumann)

Two 300kHz RDI-L-ADCP units were mounted to the CTD-Rosette for almost all casts (except 41 to 45). Initially the downward looking instrument was the SN 11436 (master) and the upward looking was SN 11461 (slave). After cast 20 it was decided to change the master (11436) because of weak beam, with a replacement instrument SN 6468. Because 6468 was in a sentinel housing the rosette was made heavier by adding weights to it.

The ADCP instruments worked in a joint mode via the same battery supply (design GEOMAR). Batteries were typically exchanged when the voltage level dropped below 42V which was about every 11th cast (Table 5.3)

Cast	Voltage before change (according to Deck box)	Voltage after change (according to Deck box)	Voltage according to processing (before change)
2	40,4	54,5	n.a.
11	43,3	54,2	n.a.
22	46,1 (before cast)	53,2	43,6
33	42,4	54,8	44,8
46	43,9	54,1	46,0
55	41,9	55,6	43,8
63	42,4	55,4	n.a.

Table 5.3 Battery changes and associated voltage changes during R/V METEOR M96. Note, before cast 21, the voltage could not be detected by the routine; after the change of the master LADCP it worked

Overall the system worked well and gave reasonable ranges (see also table 5.2). During cast 7 a power shutdown on the ship interrupted the CTD unit as well as the GPS data synchronization, which probably impacts the quality of the current profile solution. At cast 18 the CTD hit the sea floor and the processing routine reports a maximum depth of the device 2m below the bottom depth. A number of casts show that observations were made very close (<5m) to the sea floor, namely cast 5, 12, 13, 18.

For the casts that were expected to reach depth larger 6000m (st. 41 to 45) the LADCP system was removed as it was pressure rated for 6000m only. At cast 54 the data transmission from LADCP to the computer did not work and the cable and deck box were replaced. The Figure 5.3.1 shows the horizontal velocity components over the section and Figure 5.5 shows the target strength at near bottom which might be compared with the UVP results on particle concentrations.

Data processing was done with the processing routine v10.4 provided by G. Krahnemann, GEOMAR. For the processing apart from the LADCP data, navigational data from the DSHIP database was used as well as processed ship ADCP data and pre-processed CTD 1sec data files.

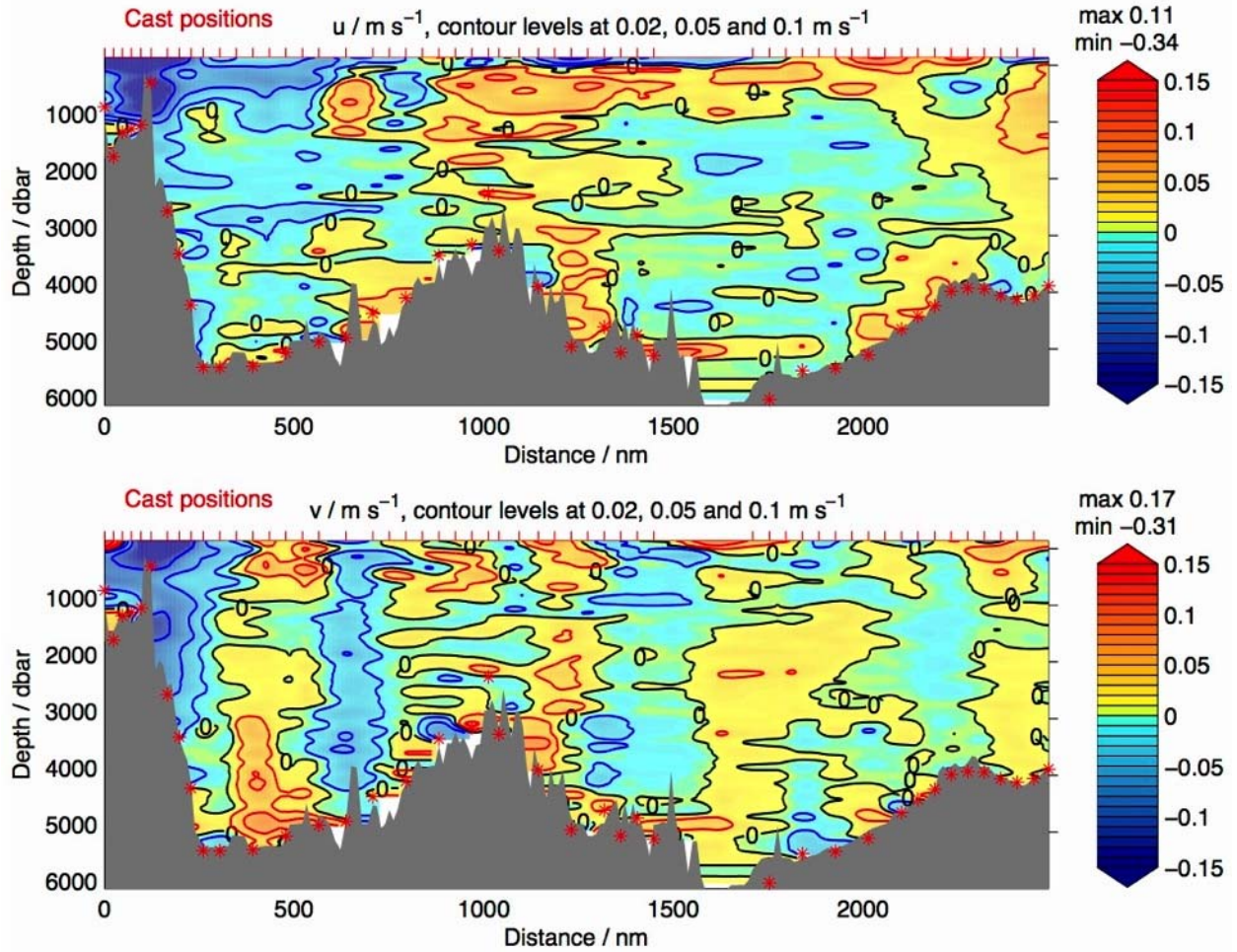


Fig. 5.5 Zonal and meridional velocity components from ADCP casts (indicated by red ticks).

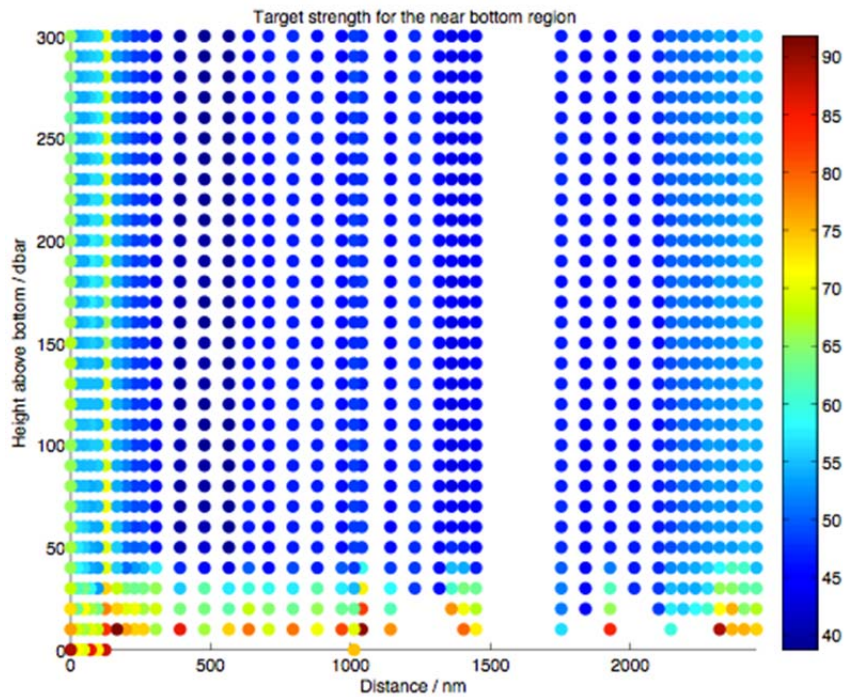


Fig. 5.6 Target strength close to the bottom

Cast	Comment
#7	power outage (CTD cast canceled) ->nosadcp data available (may had an impact on IADCP profile solution)
#8	Processing software: beam 1,3,4_up broken
#11,12	Processing software: beam 2_dn weak
#13 to 20	Processing software: beam 2_dn broken
#18	Contact with sea-floor bottom
#18 after cast	Moved weights from UVP-side of rosette to opposite side
#21	Downward looking ladcpexchanged (had also an impact on battery status in processing software)
#from 21	Noisy tilt during the downcast (new downward looking ladcp is much smaller/lighter)
#22, 24, 32, 34, 36, 38, 39, 40, 47, 49, 51, 53, 55	Processing software: beam 3_dn weak
#41 to 45	No IADCP -> max depth above pressure rating of IADCP system
#52	Data download took very long. Data from up- and downward looking instruments was recovered separately and (052.old) and copied into the 052 directory.
#54	Problems connecting to the LADCPs (tried to erase, but only produced „!!!!“. No error message. The connection unit („Deck-Box“ and the associated wire) was changed and the problem was solved.

Table 5.4 Comments on IADCP observations in relation to CTD casts

5.4 Thermosalinograph Measurements of near surface hydrography

(Michael Schlundt, Anastasia Boisgard)

During the cruise sea surface temperature (SST) and sea surface salinity (SSS) were measured autonomously as part of the Thermosalinograph (TSG).

The TSG is composed from an inlet at the front of the vessel where seawater is pumped in from outside and where temperature is sampled autonomously and a second device in the vessel's interior where temperature and conductivity are sampled. The water inlet in the ship's hull lies about 6.5 m below sea surface. At this point one SBE38 temperature sensor is installed to record what is considered "sea surface temperature". The "sea surface salinity" is analysed inside the TSG by using the SBE21 Conductivity sensor and an additional SBE38 temperature sensor inside.

Water temperature ranged between 22.9° C and 28.1° C (Figure 5.7) with a mean of 26.3°. Salinity ranged from fresher water with a mean of 35.4 in the beginning of the cruise and increased from the 5th of May to values up to 36.7 with a mean of 36.3. Moreover, salinity and temperature were compared with the calibrated CTD measurements (Figure 5.8). The upper panel compares the difference between the intake thermometer and the CTD measurements at the same water depths. The lower panel compares the salinities. The difference between TSG temperatures and the corresponding CTD value is small with a bias of ~0.005 K but some outliers could be also identified. Salinities as measured by the TSG show a constant bias (TSG minus CTD) of around 0.1 over the whole section. The reason for this offset is actually not known.

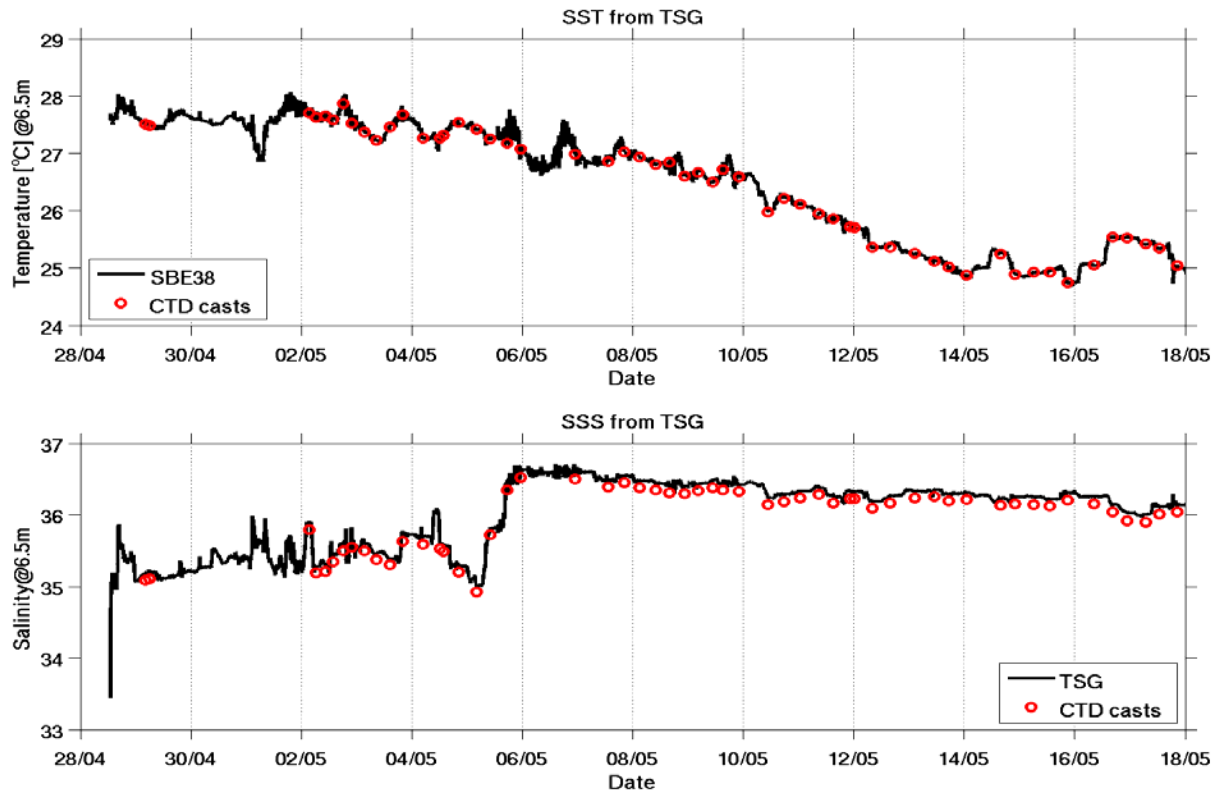


Fig. 5.7 Upper panel: Sea surface temperature as measured by the TSG. Lower panel: Sea surface salinity measured by TSG. Circles denote time were a CTD station was done (for positions see Figure 3.1.).

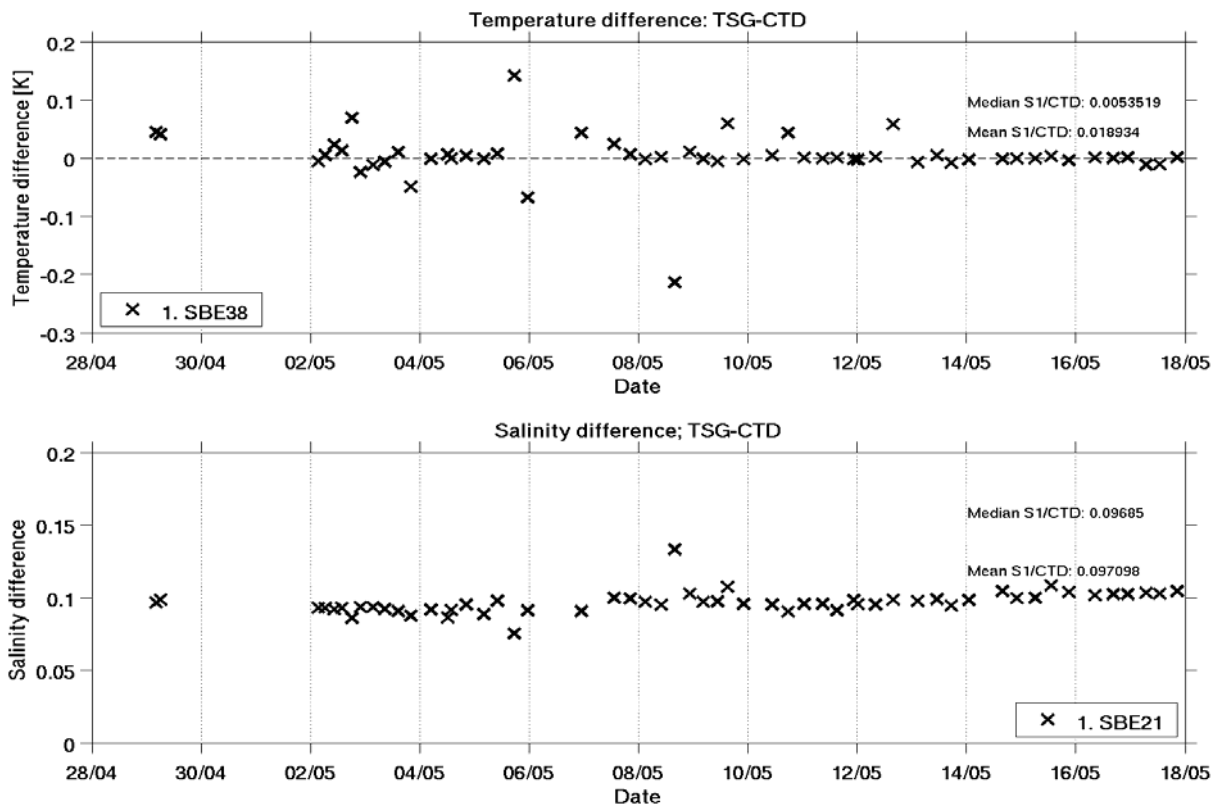


Fig. 5.8 Comparison of temperatures (top) and salinities (bottom) of the TSG system with the calibrated CTD data between 6 and 7dbar.

5.5 Mooring Operations

(Matthias Lankhorst, Scripps Institution of Oceanography)

During R/V METEOR expedition M96 three moorings which are part of the MOVE project (Meridional Overturning Variability Experiment) were serviced. MOVE was originally a German project funded by BMBF, and is now a US project funded by NOAA. The principal investigator is Uwe Send from the Scripps Institution of Oceanography, La Jolla, CA, USA. The project deployed the first instruments in 2000, and measures the southward component of the Atlantic meridional overturning circulation, a series of large-scale currents that are important components of the climate system. The technical background of the measurements is given by Kanzow et al. (2006), and more recent science results have been published by Send et al. (2011). The project maintains a website at: http://mooring.ucsd.edu/projects/move/move_intro.html. The following people participated for the MOVE project: Christian Begler, Anastasia Boisgard, Romain Heux (in-port preparations in Guadeloupe only), Matthias Lankhorst, Sung Hyun Nam.

In total, three long-wire moorings were re-deployed, and two pressure inverted echo sounders (PIES) were deployed. The long-wire moorings consist of an anchor and a riser structure composed of wire, chain and flotation elements. They contain science instruments clamped onto the wire, which measure ocean currents, temperature and salinity. The total riser lengths are shorter than the water depths, such that the entire structures remain underwater. The bottom landers consist of tripods that hold PIES instruments (pressure-sensing inverted echo sounders) made by the University of Rhode Island, USA. PIES measure pressure and acoustic travel time of a sound signal emitted to the sea surface and reflected back. There already were two PIES near the locations where the new ones were deployed, one at each site such that with the new deployments, each site is now occupied by two PIES for redundancy. All platforms also carry acoustic modems made by Teledyne Benthos that allow for communication with the instruments while they are actively on mission, e.g. for preliminary data retrieval or command control over the instruments.

PIES Deployments

For deployment, the PIES assemblies on their tripods were lowered into the surface water using the stern A-frame, and the instruments were then released to fall freely to the seafloor. Table 5.5 lists some technical details of the deployments, including the ship positions at drop time.

Site	MOVE 1	MOVE 3
Deployment date & time (UTC)	2013-5-06 14:07	2013-4-29 20:47
Ship position at deployment	15° 27.00' N 51° 31.65' W	16° 20.30' N 60° 29.33' W
PIES serial number	237	238
Acoustic modem ID	17	13

Table 5.5 Summary of PIES deployments during M96

Mooring Recoveries

The three moorings were recovered (Table 5.6. to 5.8) by acoustically triggering the release mechanisms that separate the risers from the anchors, and then by collecting the drifting mooring

components off the surface. The anchors are expendable. Recovery of mooring MOVE 1-10 was uneventful. Recovery of mooring MOVE 3-10 was made difficult by late sighting of the drifting parts, but uneventful once the mooring components had been located. Later analyses showed that the mooring was probably subject to a strong underwater current, and therefore surfaced further away from the ship than expected. Retrieval of mooring MOVE 4-10 was made difficult by foreign objects (broken fishing nets, plastic rope) entangled with the riser structure, but the mooring was ultimately recovered with minor damage to the flotation elements and no obvious impacts on the science data or instruments. The amount of objects entangled in the mooring was remarkable given that the uppermost mooring elements were well below 1000 m depth. All three moorings had been deployed from a US ship in December 2010.

The following tables list the key data of the mooring recoveries. The “science data type” columns indicate the parameters measured for the primary science data products (the instruments measure additional parameters for housekeeping and engineering purposes; the velocity instruments also measure pressure and temperature, but with low accuracy):

- C, T (, P): Conductivity, Temperature, Pressure
- Vel: Current velocity (speed and direction)

Mooring Name: MOVE1-10					Deployment Date: 2010-12-12	
Nominal Position: 15° 27.00' N 51° 30.50' W					Recovery Date: 2013-05-06	
Instrument Make	Model	Serial No.	Nominal Depth [m]	Science Data Type	Approx. Data Return	Remarks
Sea-Bird Electronics	SBE-37IM	7993	45	C, T, P	100%	
Sea-Bird Electronics	SBE-37IM	6977	90	C, T	100%	
Sea-Bird Electronics	SBE-37IM	6978	140	C, T	100%	
Sea-Bird Electronics	SBE-37IM	7994	237	C, T, P	100%	
Sea-Bird Electronics	SBE-37IM	5113	387	C, T	100%	
Sea-Bird Electronics	SBE-37IM	6361	587	C, T, P	100%	
Sea-Bird Electronics	SBE-37IM	5130	838	C, T	100%	
Sea-Bird Electronics	SBE-37IM	5118	1088	C, T, P	100%	
Sea-Bird Electronics	SBE-37IM	5131	1349	C, T	100%	
Sea-Bird Electronics	SBE-37IM	6363	1618	C, T, P	100%	
Sea-Bird Electronics	SBE-37IM	5132	1898	C, T	100%	
Sea-Bird Electronics	SBE-37IM	6364	2179	C, T, P	100%	
Sea-Bird Electronics	SBE-37IM	5133	2500	C, T	100%	
Sea-Bird Electronics	SBE-37IM	5106	2819	C, T	50%	C sensor blocked, bad data. T is ok.
Sea-Bird Electronics	SBE-37IM	6362	3139	C, T, P	100%	
Sea-Bird Electronics	SBE-37IM	6347	3460	C, T	85%	Battery empty Feb. 2013
Sea-Bird Electronics	SBE-37IM	6348	3780	C, T	100%	
Sea-Bird Electronics	SBE-37IM	7376	4100	C, T	100%	
Sea-Bird Electronics	SBE-37IM	7377	4370	C, T	100%	
Sea-Bird Electronics	SBE-37IM	5950	4640	C, T	100%	
Sea-Bird Electronics	SBE-37IM	6366	4926	C, T, P	100%	

Table 5.6 Inventory of recovered mooring M1

Mooring Name: MOVE3-10					Deployment Date: 2010-12-14	
Nominal Position: 16° 20.30' N 60° 30.30' W					Recovery Date: 2013-04-29	
Instrument Make	Model	Serial No.	Nominal Depth	Science Data Type	Approx. Data Return	Remarks

			[m]			
Sea-Bird Electronics	SBE-37IM	7995	41	C, T, P	100%	
Sea-Bird Electronics	SBE-37IM	5105	90	C, T	100%	
Sea-Bird Electronics	SBE-37IM	5939	141	C, T	100%	
Sea-Bird Electronics	SBE-37IM	6359	239	C, T, P	100%	
Sea-Bird Electronics	SBE-37IM	5940	389	C, T	100%	
Sea-Bird Electronics	SBE-37IM	5124	590	C, T, P	100%	
Sea-Bird Electronics	SBE-37IM	5949	840	C, T	100%	
Sea-Bird Electronics	SBE-37IM	7000	1091	C, T, P	100%	
Sea-Bird Electronics	SBE-37IM	4877	1352	C, T	100%	
Nortek	Aquadopp	3026	1382	Vel	100%	Serial no. is for acoustic head
Sea-Bird Electronics	SBE-37IM	5953	1621	C, T, P	100%	
Sea-Bird Electronics	SBE-37IM	5942	1902	C, T	100%	
Sea-Bird Electronics	SBE-37IM	5955	2183	C, T, P	100%	
Sea-Bird Electronics	SBE-37IM	5943	2504	C, T	100%	
Sea-Bird Electronics	SBE-37IM	5957	2823	C, T, P	100%	
Nortek	Aquadopp	3025	2993	Vel	100%	Serial no. is for acoustic head
Sea-Bird Electronics	SBE-37IM	5944	3144	C, T	100%	
Sea-Bird Electronics	SBE-37IM	5946	3464	C, T	100%	
Sea-Bird Electronics	SBE-37IM	4518	3785	C, T, P	100%	
Sea-Bird Electronics	SBE-37IM	5947	4104	C, T	100%	
Sea-Bird Electronics	SBE-37IM	5948	4375	C, T	100%	
Sea-Bird Electronics	SBE-37IM	5941	4645	C, T	100%	
Sea-Bird Electronics	SBE-37IM	5958	4931	C, T, P	100%	

Table 5.7 Inventory of recovered mooring M3

Mooring Name: MOVE4-10				Deployment Date: 2010-12-15		
Nominal Position: 16° 21.75'N 60° 36.45'W				Recovery Date: 2013-04-28		
Instrument Make	Model	Serial No.	Nominal Depth [m]	Science Data Type	Approx. Data Return	Remarks
Nortek	Aquadopp	2951	1335	Vel	100%	Serial no. is for acoustic head
Nortek	Aquadopp	3024	2237	Vel	100%	Serial no. is for acoustic head

Table 5.8 Inventory of recovered mooring M4

Mooring deployments

To replace the three recovered moorings, three new ones were deployed (Table 5.9 to 5.10). The mooring structures were paid out over the stern using the ship A-frame, starting from the top, while the ship was steaming into the wind and waves at 1 to 1.5 knots through water. The anchors were dropped after passing over the nominal positions and overshooting these by approximately ¼ of the mooring riser lengths. The initial distances from the mooring positions at the start of operations had been budgeted that there would be 6, 6, and 4 hours time for work until reaching the target positions; the actual times needed were about 5, 6, and 2 hours (sites MOVE 1, 3, and 4, respectively). The science data types are identical to the recovered moorings.

Mooring Name: MOVE1-11			Deployment Date: 2013-05-06		
Nominal Position: 15° 27.00' N 51° 30.50' W					
Instrument Make	Model	Serial No.	Nominal Depth [m]	Science Data Type	Remarks
Sea-Bird Electronics	SBE-37IM	7995	57	C, T, P	
Sea-Bird Electronics	SBE-37IM	5105	102	C, T	
Sea-Bird Electronics	SBE-37IM	5939	152	C, T	
Sea-Bird Electronics	SBE-37IM	6359	246	C, T, P	
Sea-Bird Electronics	SBE-37IM	5940	396	C, T	
Sea-Bird Electronics	SBE-37IM	5124	597	C, T, P	
Sea-Bird Electronics	SBE-37IM	5949	847	C, T	
Sea-Bird Electronics	SBE-37IM	7000	1104	C, T, P	
Sea-Bird Electronics	SBE-37IM	4877	1355	C, T	
Sea-Bird Electronics	SBE-37IM	5953	1605	C, T, P	
Sea-Bird Electronics	SBE-37IM	5942	1842	C, T	
Sea-Bird Electronics	SBE-37IM	5955	2143	C, T, P	
Sea-Bird Electronics	SBE-37IM	5943	2444	C, T	
Sea-Bird Electronics	SBE-37IM	5957	2744	C, T, P	
Sea-Bird Electronics	SBE-37IM	5944	3054	C, T	
Sea-Bird Electronics	SBE-37IM	5946	3374	C, T	
Sea-Bird Electronics	SBE-37IM	4518	3695	C, T, P	
Sea-Bird Electronics	SBE-37IM	5947	4014	C, T	
Sea-Bird Electronics	SBE-37IM	5948	4335	C, T	
Sea-Bird Electronics	SBE-37IM	5941	4655	C, T	
Sea-Bird Electronics	SBE-37IM	5958	4914	C, T, P	

Table 5.9 Configuration of deployed mooring M1

Mooring Name: MOVE3-11			Deployment Date: 2013-04-30		
Nominal Position: 16° 20.30' N 60° 30.30' W					
Instrument Make	Model	Serial No.	Nominal Depth [m]	Science Data Type	Remarks
Sea-Bird Electronics	SBE-37IM	5114	38	C, T, P	
Sea-Bird Electronics	SBE-37IM	5109	87	C, T	
Sea-Bird Electronics	SBE-37IM	5110	137	C, T	
Sea-Bird Electronics	SBE-37IM	5115	234	C, T, P	
Sea-Bird Electronics	SBE-37IM	6986	384	C, T	
Sea-Bird Electronics	SBE-37IM	5119	585	C, T, P	
Sea-Bird Electronics	SBE-37IM	5259	835	C, T	
Sea-Bird Electronics	SBE-37IM	5122	1092	C, T, P	
Sea-Bird Electronics	SBE-37IM	5357	1343	C, T	
Nortek	Aquadopp	3026	1373	Vel	Serial no. is for acoustic head
Sea-Bird Electronics	SBE-37IM	5700	1594	C, T, P	
Sea-Bird Electronics	SBE-37IM	5358	1831	C, T	
Sea-Bird Electronics	SBE-37IM	5701	2132	C, T, P	
Sea-Bird Electronics	SBE-37IM	5698	2433	C, T	
Sea-Bird Electronics	SBE-37IM	5956	2734	C, T, P	
Sea-Bird Electronics	SBE-37IM	5945	3043	C, T	
Nortek	Aquadopp	3028	3123	Vel	Serial no. is for acoustic head
Sea-Bird Electronics	SBE-37IM	5357	1343	C, T	
Nortek	Aquadopp	3026	1373	Vel	Serial no. is for acoustic head
Sea-Bird Electronics	SBE-37IM	5700	1594	C, T, P	
Sea-Bird Electronics	SBE-37IM	5358	1831	C, T	
Sea-Bird Electronics	SBE-37IM	5701	2132	C, T, P	
Sea-Bird Electronics	SBE-37IM	5698	2433	C, T	
Sea-Bird Electronics	SBE-37IM	5956	2734	C, T, P	
Sea-Bird Electronics	SBE-37IM	5945	3043	C, T	
Nortek	Aquadopp	3028	3123	Vel	Serial no. is for acoustic head
Sea-Bird Electronics	SBE-37IM	5128	3364	C, T	

Sea-Bird Electronics	SBE-37IM	5126	3685	C, T, P	
Sea-Bird Electronics	SBE-37IM	6988	4004	C, T	
Sea-Bird Electronics	SBE-37IM	6989	4325	C, T	
Sea-Bird Electronics	SBE-37IM	6990	4645	C, T	
Sea-Bird Electronics	SBE-37IM	5959	4904	C, T, P	

Table 5.10 Configuration of deployed mooring M3

Mooring Name: MOVE4-11			Deployment Date: 2013-04-30		
Nominal Position: 16° 20.00' N 60° 36.45' W					
Instrument Make	Model	Serial No.	Nominal Depth [m]	Science Data Type	Remarks
Nortek	Aquadopp	2999	1341	Vel	Serial no. is for acoustic head
Nortek	Aquadopp	3022	2242	Vel	Serial no. is for acoustic head

Table 5.11 Configuration of deployed mooring M4

Instrument Calibration

The SBE-37 instruments on the MOVE1 and MOVE3 moorings were field-calibrated prior to deployment and after recovery. For this procedure, the instruments are attached to the ship-board CTD rosette system, and a CTD cast is carried out during which the mooring instruments sample every few (typically 10) seconds. On the up-casts, the rosette is stopped at multiple depths for several minutes. Data from these stops are then extracted and used to determine calibration adjustments for the mooring instruments based on comparison against the ship-board system. During the R/V METEOR M96 expedition, this occurred during the following CTD casts:

- 1, 2 (MOVE3-11 pre-deployment)
- 12, 14, 15 (MOVE1-11 pre-deployment and MOVE3-10 post-recovery)
- 33, 34, 37 (MOVE1-10 post-recovery)

With the adjustments thus derived, a preliminary version of the data was created on board that passed QC inspection by M. Lankhorst. For this purpose, the following ship-board CTD sensors were used as true references:

- Conductivity: use CTD sensor 1, adjust by multiplying with 1.000027
- Temperature: use CTD sensor 1, no adjustments to CTD data
- Pressure: use the only CTD sensor, no adjustments to CTD data

The above adjustment to the CTD conductivity data was based on a preliminary analysis of the salinometer data, and results in very minor adjustments to the salinity that are smaller than the nominal accuracy of the CTD system.

For information on data access see chapter 8 of this report.

5.6 Biogeographical distribution and activity of diazotrophs

(Julien Dekaezemaker, Clara Martinez Pérez, Laura Piepgras, Wiebke Mohr)

The main objectives of the biogeochemical program was to assess the activity, abundance and diversity of diazotrophic microorganisms and the determination of the rates of primary production and dinitrogen (N₂) fixation along a trans-Atlantic transect at 14°30'N in regard of nutrient availability and Saharan dust deposition. Regular ~24-h time interval samples during ship's steaming time, provided a ~3° latitude horizontal resolution enabling the assignment of biogeographical regions for the different diazotrophic groups to be analysed. The N₂ fixation

rates and the analysis of *nifH* gene expression patterns will be correlated to environmental conditions such as temperature, light, nutrient availability and Saharan dust deposition. The molecular analysis will be supplemented with analytical flow cytometry samples and proteomic samples as well as the determination of rates of N₂ fixation and primary production from the community scale (bulk measurements) to the cellular scale (nanoSIMS analysis), using the stable isotopes ¹⁵N₂ and NaH¹³CO₃, respectively. The overall data set will provide a spatial (both horizontal and vertical) and temporal distribution of the activity and abundance of diazotrophs throughout the North Tropical Atlantic Ocean.

Cruise experiments

The first seawater samples using the Niskin bottles of the CTD were obtained in the early morning on the 1 May 2013. From thereon, samples were taken daily throughout the cruise until 19 May 2013. In summary, a total of 14 stations were sampled for the determination of rates of N₂ fixation and primary production and for the molecular analysis of the diazotrophic community during the cruise. Samples were taken from daily (~midnight) CTD casts including 6 depths covering the upper 200 m of the ocean. The sampling depths were distributed throughout the water column and were adjusted according to the chlorophyll *a* fluorescence maximum, the abundance of particles or hydrographical features. 28 stations were also sampled for the determination of the nutrients (NO₃⁻, NO₂⁻, NH₄⁺, PO₄³⁻) concentrations.

On-deck 24-h seawater incubations were performed to determine rates of N₂ fixation and primary production using the stable isotopes ¹⁵N₂ and NaH¹³CO₃, respectively. In specific, triplicate 4-L polycarbonate bottles were filled with seawater from the night CTD cast. The stable isotopes were added to the bottles, which were placed in an on-deck incubator with ambient surface seawater flow-through for about 24 h. Non-amended seawater incubations for the analysis of the natural abundance of ¹⁵N, and ¹³C were included during each incubation. After the incubation time, the samples were filtered onto pre-combusted GF/F filters, dried at ~ 50°C and stored at room temperature until bulk mass spectrometric analysis.

In addition, seawater samples (usually about 2 l) were filtered onto Durapore membrane filters (0.22 µm pore size, 47 mm diameter), shock-frozen in liquid nitrogen and stored at -80°C until further analysis in the molecular laboratory at the GEOMAR in Kiel (collaboration with Caroline Löscher). To supplement the molecular analysis, analytical flow cytometry (AFC) and fluorescence in situ hybridization (FISH) samples were taken in parallel to the seawater filtrations for determining the abundance and the diversity of diazotrophs.

Finally, samples for proteomics were taken using In-situ Pumps which have been deployed at four stations across the transect in order to filter large volumes of seawater at the deep chlorophyll maximum (~1300 L/station). At ten stations, surface seawater samples were obtained by using the ship's clean seawater supply (~235 L/station)

Preliminary/Expected Results

The daily CTD casts down to 200 m depth will provide an insight into the vertical distribution of the activity and the presence of different diazotrophic groups. The conjunction of the horizontal and vertical distribution will reveal biogeographical information of diazotrophs throughout the Atlantic Ocean including areas of highest dust deposition, *i.e.* the Eastern North Atlantic. While

passing this area, atmospheric dust could be observed from the ship. The first measurements of nutrients (NH_4^+ and NO_2^-) showed concentrations mostly below detection limit but dust has previously been shown to stimulate N_2 fixation (Mills *et al.* 2004) by providing other nutrients such as iron and phosphorus to the surface ocean microbial community (Baker *et al.* 2007). Both elements are considered to be limiting nutrients for N_2 fixation. Rates of N_2 fixation and primary production will be obtained through laboratory-based mass spectrometric analysis. Using molecular biological techniques (quantitative PCR), we will also obtain abundance estimates for at least seven different phylotypes of diazotrophs using specific probes for the *nifH* gene, which encodes the iron-subunit of the nitrogenase enzyme complex. *NifH* gene expression analysis on these samples will reveal (potential) activity patterns of diazotrophs during the cruise, providing a horizontal and temporal distribution of the abundance and activity of diazotrophs.

We will also analyse the distribution and natural abundance of the stable isotopes of carbon and nitrogen in proteins from the samples taken with the in-situ pumps. The natural abundance of these isotopes can reveal patterns of nutrient acquisition and utilization with respect to carbon and nitrogen sources, for example, whether organisms are exclusively photosynthetic or if they are at times exhibiting a heterotrophic lifestyle. Due to the differences in dust deposition across the Atlantic transect, we expect to see differences in carbon and/or nitrogen utilization patterns within these samples because Saharan dust can be a major source of trace metals which are essential compounds for many enzymatically-mediated biogeochemical processes.

5.7 Calipso Satellite Surveys

(Stefan Kinne, Ronny Engelmann)

During the R/V METEOR M96 expedition we had two opportunities to do an OCEANET lidar survey in parallel to a Calipso satellite lidar survey. The Calipso satellite has a profiling lidar system (Caliope) on-board measuring aerosol vertical distributions under cloud-free conditions, structures on optically thin clouds and general information on cloud top altitudes. The parallel measurements from the ship and the satellite can be of use in addressing the following questions:

- Can Calipso identify the correct aerosol type and place aerosol at the correct altitudes?
- Can Calipso data identify cloud-structures at the correct locations?

Such validation comparisons are complicated by the tiny spatial pixels offered by (non-scanning) nadir views of the satellite, which makes the time and space match of the observation from both systems very limited.

	Latitude	Longitude	UTC	UTC
Point 1	14 00.00 N	44 05.64 W	0.14	6.00
Point 2	14 06.00 N	44 06.96 W	0.45	5.13
Point 3	14 12.00 N	44 08.34 W	1.16	4.26
Point 4	14 18.00 N	44 09.60 W	1.45	3.40
Point 5	14 24.00 N	44 11.04 W	2.16	2.54
Point 6	14 27.00 N	44 11.76 W	2.32	

Table 5.11 RV METEOR M96 ship track information during the Calipso overpass.

For the comparison, a night time overpass was desirable to minimize interference by radiation from the sun. Such a rare opportunity occurred (see table 5.11) during the night from May 9 to

May 10, shortly after 00:00 UTC. The ship was manoeuvred on May 10 to follow (at full speed, 11 kn) a track along the ground projection of the CALIPSO track over a distance of almost 50km. The ship then returned (at reduced speed, 8 Kn) on the same path back to the 14.5N/44W at 06:00 UTC. The actual Calipso overpass was calculated to occur during the return leg, at 04:46 UTC (14.162 N/44.138 W).

During both ship-legs continuous ship-borne IR brightness temperature recorded an intermitted coverage by low clouds, which appeared more frequent during the return leg. Otherwise cloud-free conditions dominated as stars in the sky were visible - except when obscured low passing small size low altitude cloud elements (e.g. trade wind cumuli). Conditions at the water level were rather humid as the water temperature (26.5 C) was higher than the temperature of the air (25.7 C). Data of the May 10 radio sonde profile are listed in Figure 5.10. Also presented are DWD back-trajectories at 750hPa (~ 3000m) and at 850hPa (~1000m), which indicate transport of air from regions of the Western Sahara. Thus, due atmospheric dust loading during this time of the year, elevated dust aerosol can be expected along the overpass track.

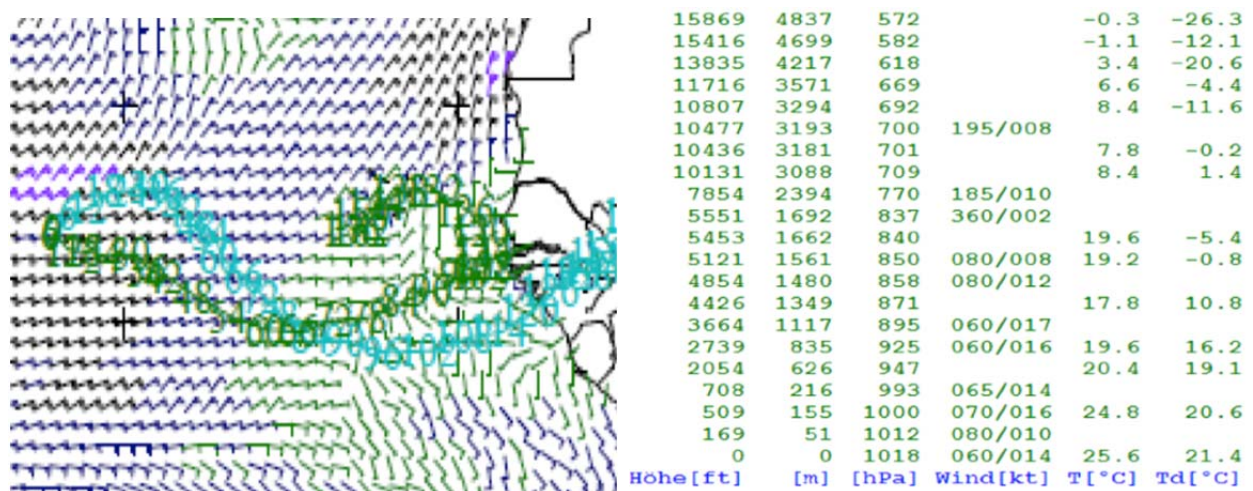


Fig.5.9 Radiosonde and DWD back trajectories for May10, 0 UTC at 850 (blue) and at 700 hPa green)

The map location of the track points of Table 5.11 and selected IR images when passing different track points on the southward and the northward ship-leg are presented in Figure 5.10.

The corresponding 00:00-06:00 UTC time-series of the ship-borne lidar data (not shown) show vertical profiles of atmospheric backscattering at 532 and 1064 nm wavelengths and the depolarization signal at 532 nm. Hereby, elevated backscatter signals indicate the presence of atmospheric particles (and larger particles such as cloud droplets or dust aerosol are better contrasted at the larger 1064 nm wavelength). Elevated depolarization values indicate the presence non-spherical particles such as (crystals of) high altitude (cirrus) clouds and dust aerosol.

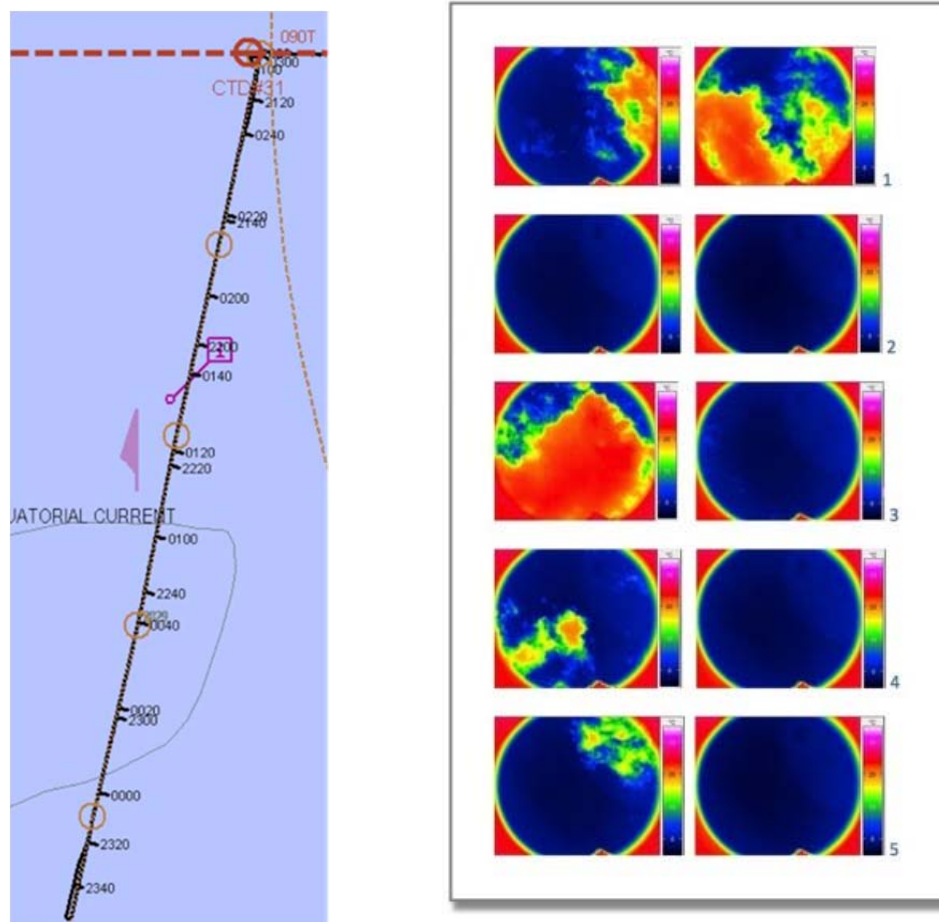


Fig. 5.10.: (left) Track and local times (UTC+3hrs) of RV METEOR during the clipso survey 1 along a-Train formation track with overpass at 04:46 UTC on 10 May 2014. (right) Selected IR temperature images, when passing Points 1 to 5 for both, the southward (images to left) and the northward direction track (images to the right).

The ship-borne lidar data identified a consistent elevated dust aerosol layer between 1.5 and 3.5 km altitude and intermitted lower altitude cloud cells. The image of the southward track (00:14-02:16 UTC) is not a mirror image of the northward track (02:54 – 06:00) UTC, which had to be expected with time-differences ranging between 40 minutes (at Point 5) to almost 6 hours (at Point 1). As observed, the frequency of low altitude trade-wind cumulus cloud events (with a cloud base near 500m) increased on the later northward (return) track. The identified (bipolarisation and elevated backscatter, especially at 1064nm) dust-layer was more stable on the northward return leg.

These ship-based lidar data are intended to be used as reference for the Calipso lidar data from space. However for the following comparisons, it should be noted that Calipso data are averaged over 5km (e.g. low level intermittent clouds are interpreted as overcast) and also that at distances further away from the direct overpass at (14.162N/44.138W) advection related changes will introduce noise.

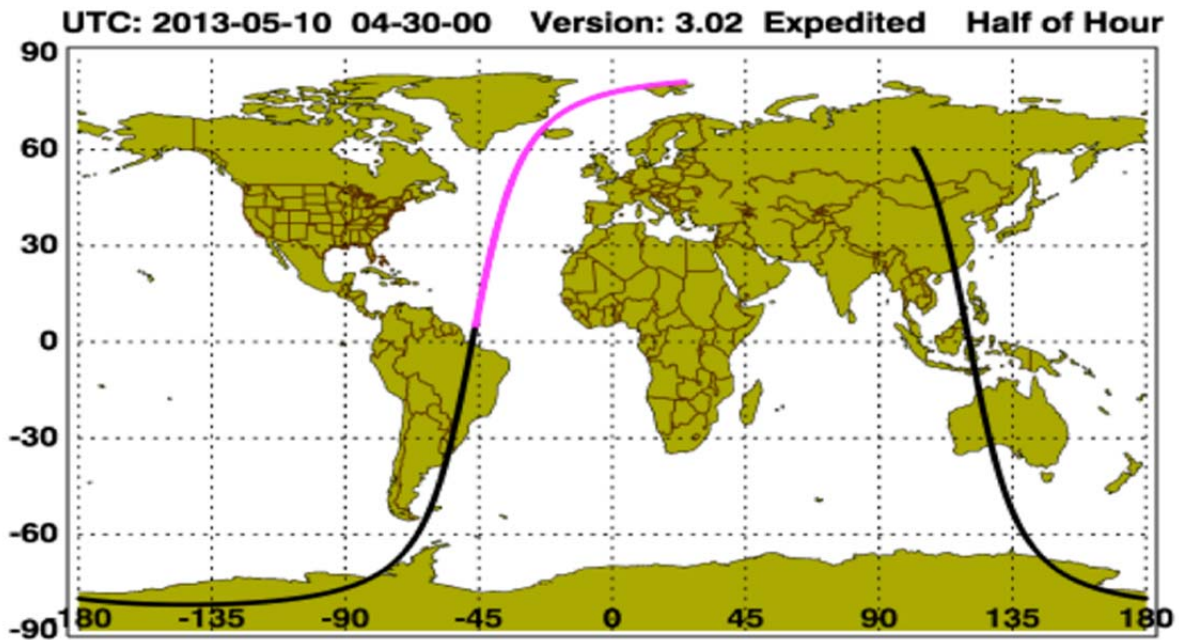


Fig. 5.11 Night-time track of the space-borne CALIPSO lidar on May 10.

The ca 50km in reference track data provided by the ship-borne lidar (in about 3 hours) is passed by the satellite in about 5 seconds and covers only a tiny portion of its entire track segment (Figure 5.11). Thus, aside from data for the entire segment there is interest to examine satellite retrieved data for the matching reference track. This portion is extracted and enlarged for direct comparison to the lidar data.

The detected atmospheric particles are classified as function of altitude and which also offers an aerosol type classification (Figure 5.12). Preliminary analysis on the ship showed that Calipso detected low altitude clouds and aerosol as observed on the ship. Near the surface marine aerosol were identified (when no low clouds are present) and above the low clouds an elevated layer of dust was detected. This identification agrees well with the ship-borne lidar data. Even the altitude assignment for the aerosol types is excellent, as the elevated dust layer is placed between 1.5 and 3.5 km. Still, when comparing the altitude assignment for aerosol type and backscatter there is some apparent altitude disagreement. The backscatter data are placed almost 1 km lower in the atmosphere with most low-level clouds positioned at negative (!) altitudes. It is not clear, if this is an altitude model problem or just a quick-look plotting error. Aside from this altitude problem, though there is excellent agreement to the ship-borne lidar data (considering that the horizontal resolution of the Calipso product is (at 5km) much coarser than the ship-borne data. The validation effort for this particular overpass was quite encouraging: (1) Calipso identified the correct aerosol type and Calipso placed the aerosol at the correct height (2) Calipso identified correctly low altitude clouds, but could not resolve their small scales.

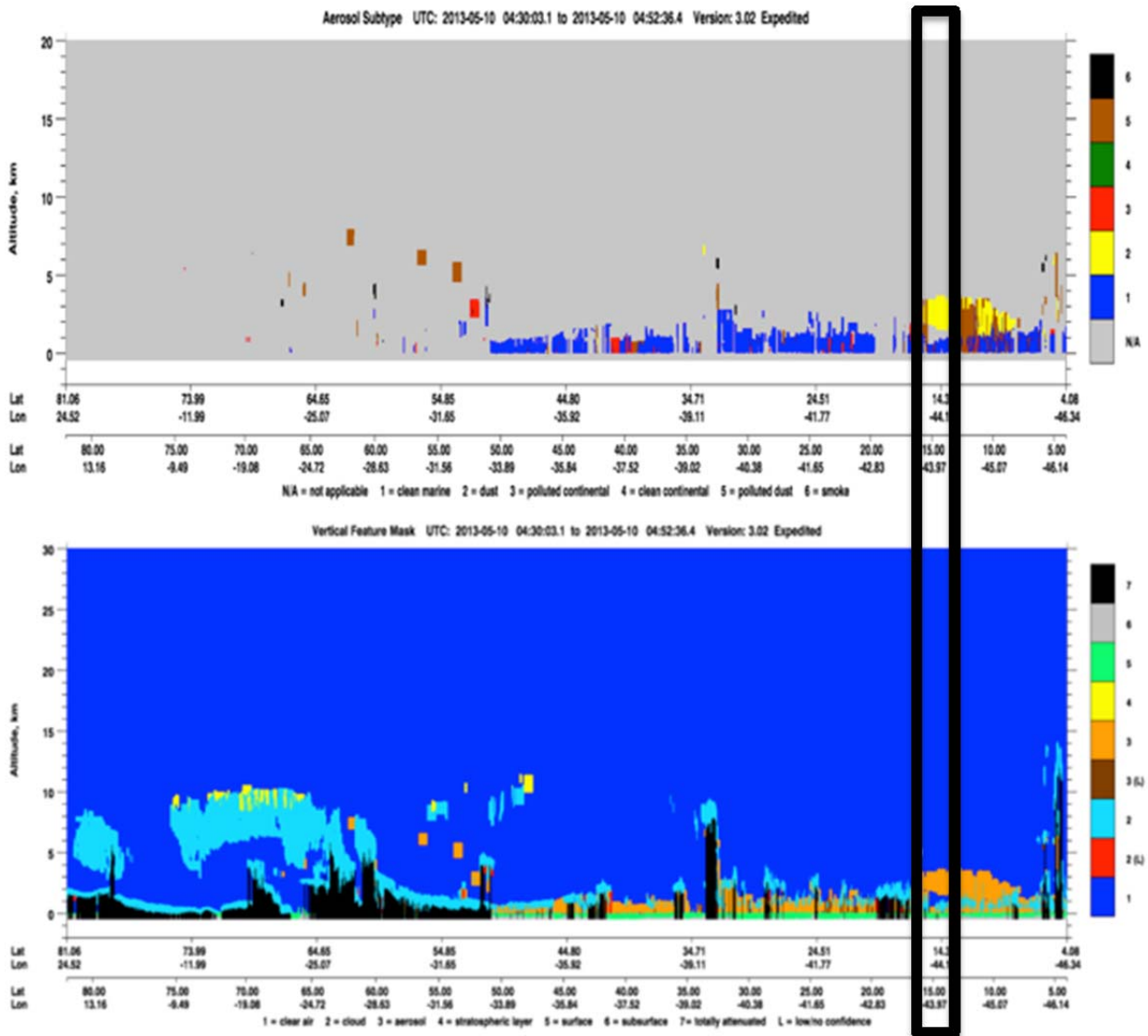


Fig. 5.12 (Upper) feature mask (light blue: cloud, orange: aerosol) and (below) identified aerosol type (blue: clean marine, yellow: dust) for the entire sub-section of the Calipso flight track and only for the validation track corresponding to the ship-borne data (black square).

5.8 The FUB Sun and Sky Photometers for Aerosol Remote Sensing

(Thomas Ruhtz, Jonas v. Bismarck, Sören Testorp)

Two scientific questions were addressed by the experiments performed by the Freie Universität Berlin (FUB) during R/V METEOR M96: (1) determination of aerosol optical properties in the atmosphere by observations with Sunphotometers and the (2) characterization of the water leaving radiance and the reflected and scattered sun light by observations with the instrument setup URMS/AMSSP. To address (1), two Sunphotometers were used by FUB: a standard transportable Sunphotometer, widely used by the Aeronet community and an instrument build by the FUB that measure, in addition to the single direct light coming from the Sun, the aureole around the Sun in two different angles. To address (2), a highly experimental setup was done with the first field deployment of the URMS/AMSSP instrument. This effort was driven by the current institute research topic on Multi-angle polarized model simulations and measurements of the water leaving radiance.

The FUB Sun and Sky Photometers for Aerosol Remote Sensing

Sun photometers allow measuring atmospheric transmissivity in the UV, visible and/or SWIR parts of the solar spectrum, if correctly calibrated. To compute the aerosol optical depth from multi- or hyper spectral transmissivity measurements, the contribution of other scatterers and absorbers, as for instance scattering at the air molecules or absorption by trace gases, have to be either estimated, taken from external sources, or derived from the spectral information from the measurements and subtracted. The devices used on the cruise allow deriving aerosol optical depth and columnar ozone and water vapour, without depending on limiting a priori assumptions. Furthermore, the spectral decrease of the aerosol optical depth allows estimating the size range of the particles by calculating the so called Angstrom parameter, and the aureole measurements reveal scattering properties of the particles in the forward scattering region, allowing an inversion of the scattered particle type.

In contrast to the ground-based remote sensing of aerosols over land, by stationary Sun photometers as for instance the CIMEL instruments at many AERONET sites around the globe, there is a lack of measurements on the oceans. Mounting aerosol remote sensing instruments on moving ships and using satellite measurements are the main approaches to fill this gap. While the satellite products provide global coverage of aerosol optical properties using complex algorithms and inversion schemes depending on a priori assumptions, direct ground based measurements with sun photometers are essential to validate the quality of these products.

The M96 expedition enabled us to measure aerosol loading along one of the main transport routes of Saharan dust, from the African continent over the Atlantic and even further to Latin America. It was expected that air masses with dust of different ages would be observed. The **FUBISS-ASA2** radiometer was originally designed for airborne remote sensing of aerosols and is therefore able to continuously correct its attitude and track the sun even in cloudy conditions, unlike many of the Sun photometers designed for ground-based use. The second sun photometer we used was a small handheld **Microtops II** unit that is commercially available and widely used for the aerosol optical depth (AOD) measurements on cruises processed and distributed by NASA/GSFC for the “AERONET Maritime Aerosol Network”. The instrument was similar to a

second Microtops unit, brought to the cruise and operated by MPI Hamburg, and provides three channels at positions also provided by our instrument. The parallel deployment of the Microtops instrumentation provided some redundancy and enabling data quality checks, and another two channels at different positions, adding spectral resolution to the combined dataset.

Microtops II

The handheld Sun photometer manufactured by SOLAR LIGHT and owned by the FUB offers five channels with different narrow spectral filters at 380nm, 500nm, 870nm, 936nm (for columnar water vapour retrieval) and 1020nm. The MPI device operated during M96 enabled measurements at 380nm, 440nm, 670nm, 870nm and 936nm. The instruments provide the operator a Sun target screen to enable accurate pointing of the instrument at the sun. The Microtops is connected to a Garmin GPS 72H device by a serial data cable to provide position and UTC time of each scan. In the settings required by the GSFC for AERONET processing, the instrument does 20 scans within approximately 8 seconds and only stores the data from the scan with the highest signal.

Calibration and Known Technical Issues

Prior to the campaign the unit was calibrated at NASA GSFC relatively to the AERONET standard unit by Alexander Smirnov. During the cruise, the data was sent to A. Smirnov at GSFC twice a week where it was processed to preliminary cloud screened level 1.5 AOD and water vapour column. Plots with level 1.5 AOD and Angstrom exponent have directly been made available by us throughout the campaign. To raise the processing level AERONET level 2 standard, the unit will be sent back to GSFC after the campaign for another calibration round. The final cloud screening, especially of hard to detect thin cirrus clouds, will be performed there by evaluation of the notes about the atmospheric conditions during the measurements and the sky photos that we shot.

During the campaign, some dust was accumulating on the window of the instrument. A couple times we blew the particles away with a dry-pressure-air can. Checking the recorded signals from before and after those cleaning processes showed a slight change only in the outermost channels (380nm and 1020nm), which was precisely documented in a log file. On 20th May, some sea spray also reached the instrument window throughout the day. A detailed analysis and the next calibration will show if there was any effect on the measured signal. Generally, a preliminary comparison of spectra measured spectra of MPI Hamburg Microtops and our Microtops device showed no significant trend or differences throughout the campaign.

FUBISS-ASA2

The Institute for Space Sciences has been developing spectral Radiometers for stationary use and for the use on moving platforms for nearly two decades. The construction of the airborne dual aureole and Sun photometer FUBISS-ASA2 (Aureole and Sun Adapter 2) has all optical components, including four spectrometers, integrated inside of the Sun tracking head. It allows measurements of direct Sun light and from two circular regions around the solar position 4° and 6° around the sun in the solar aureole. The aureole optical entrance tubes have ring shaped apertures to shield the direct sunlight and only allow radiation from the 4° and 6° scattering angle regions to pass. The monolithic miniature spectrometers used for the sun- as well as the aureole

photometers provide 256 evenly spaced spectral channels from 300 to 1000 nm. Broadband color and gray filters in the tubes of the Sun photometer optimize the incoming radiation for the dynamic range of the sensor at an integration time of about 100 ms allowing approximately 10 measurements per second. Sun tracking is achieved by the real-time evaluation of sun position signals from a four-quadrant-diode to generate commands for two Motion Controllers and rotation axes. The two orthogonal axes are enabling the rotation of the head and to point to a measured or calculated direction in the upper hemisphere to follow the Sun. Depending on platform movement, weather conditions like a cloudy sky or light obstructing elements the system can switch to calculated Sun Positions. These can be corrected by the information of GPS and inertial systems.

Prior to the campaign the so far integrated DC motors had to be swapped to more powerful step motors due to some issues with the DC azimuth round table on a prior campaign. In this step the 4 quadrant diode for solar tracking also had to be replaced due to sensor degradation of the prior unit. These two steps made some software adjustments and tests on the first 2 days of the cruise necessary, to ensure accurate Sun tracking throughout the transect, which were carried out under atmospheric conditions which would have not allowed aerosol measurements. One typical remaining issue typical for Sun photometers on moving platforms at very low solar zenith angles is the azimuth motion control when the sun is in the zenith at noon. However, data where the instrument was not directly pointing at the sun in between good measurements can be easily identified and flagged out.

To assure the quality of the retrieved aerosol optical properties, a calibration before or after a campaign is helpful. This calibration with the so called 'Langley-Plot' technique has to be performed under very stable atmospheric conditions. The last planned calibration before the cruise was supposed to be done in-flight on a research aircraft but had to be cancelled due to grounding of the aircraft for technical reasons. A comparison with the well calibrated Microtops unit (Figure 5.13) showed that for the two most important channels the Angstrom parameter was determined to be $\ln V_o(500\text{nm})=5.223$ and $\ln V_o(870\text{nm})=4.016$.

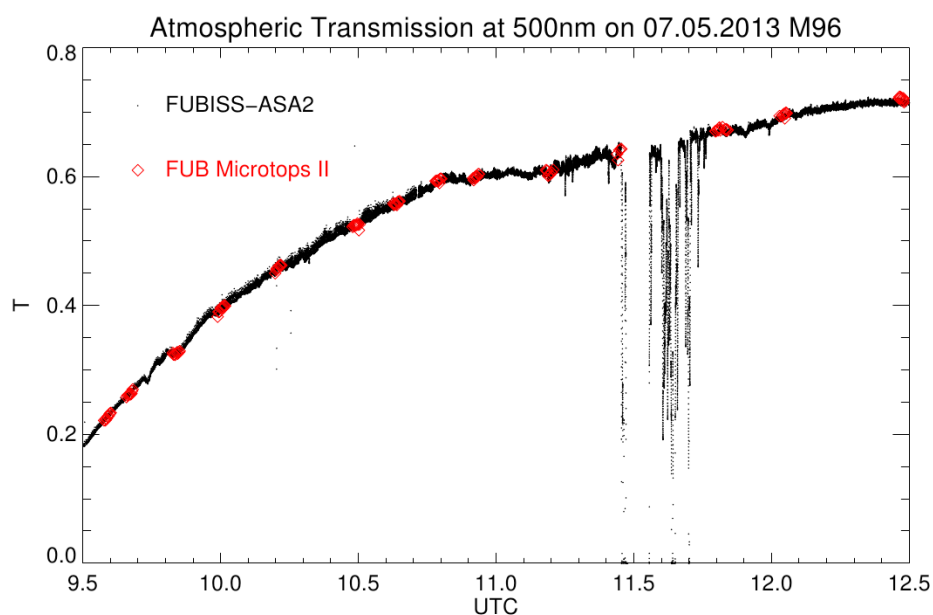


Fig.5.13

Comparison of atmospheric Transmissions derived from the FUBISS-ASA2 and Microtops measurements after a relative calibration of both instruments aboard the R/VMETEOR.

The instrument was first set up on the “Peildeck”, with the controlling units situated in the air-chemistry lab. This allowed good measurements in the first half of the day, but caused some trouble during noon and afternoon due to ropes and structures throwing a shadow on the instrument. From May 8 until May 10 a position on the starboard side of the air chemistry lab was tested. This site caused some problems with smoke track contamination of the afternoon and evening measurements. The instrument was then moved to the backboard side of the chemistry lab on May 11, which turned out to be the best position on course east, preventing smoke track contamination and only requiring one repositioning of the instrument per day by a few meters.

To prevent sea spray and accumulated dust on the entrance filter of the Sun photometer from having an influence on the measurements, the filter was cleaned every morning with ethanol. The integration time of each single measurement was limited to values not lower than 50 milliseconds if necessary for a short period of time, and not lower than 70ms over a longer period of time, due to technical limitations of the controlling PC. On rather dusty days, this sometimes led to an out of range signal for the aureole measurements. Therefore the integration time was set down to (a rather critical in terms of system stability) 50 ms from time to time for a while on these days, to have some processable aureole data.

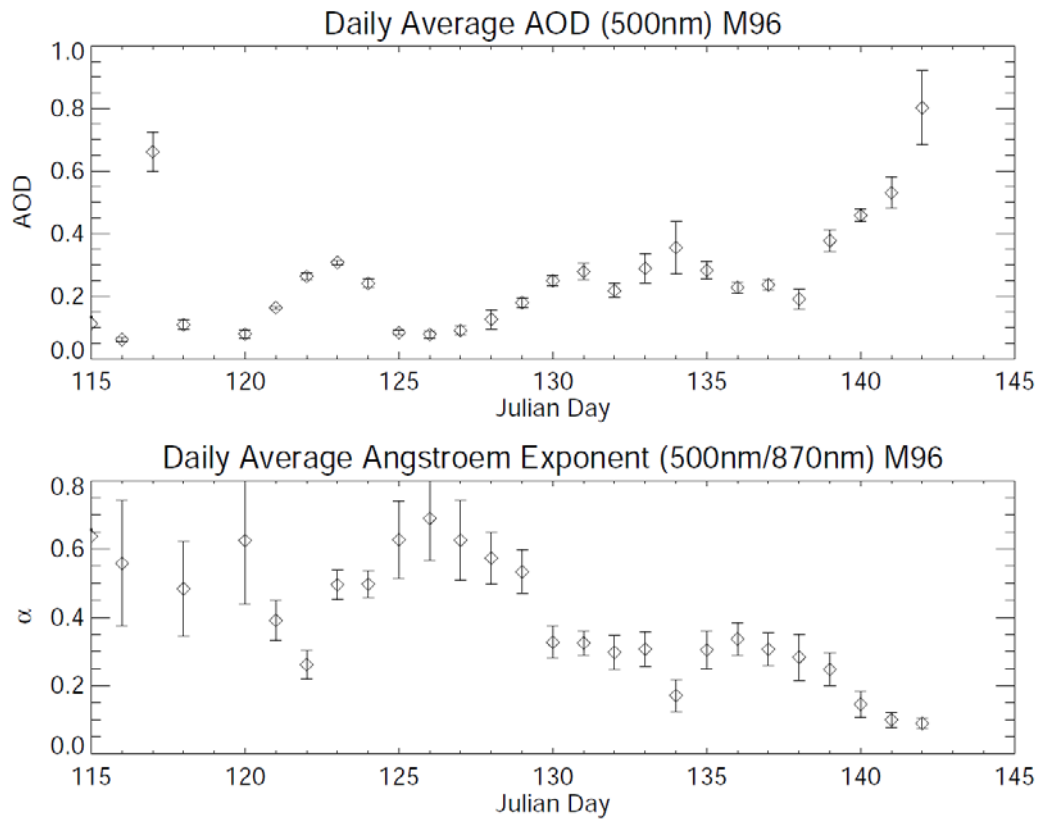
On this cruise, FUBISS-ASA2 could not be connected to a dedicated GPS device providing position data. Therefore, the time of the data logging PC was set to UTC time, to be able to use Dship GPS data for the processing. Differences to the UTC time on board in the order of a few seconds were noted in the instrument log file each day.

The raw data has been processed to WeW level 0b (NCDF Files containing the measured spectra and the motion control data) aboard the ship, to ensure usable data was produced throughout the cruise. The processing of the large amount of hyper spectral data to cloud screened level 2a aerosol products has been started on board on a laptop and will be completed on the more powerful machines at our institute after the end of the cruise.

Measurements and First Results

The atmospheric conditions on the cruise allowed measurements of AOD throughout the cruise (Figure 5.14). The only dates with no measurements are April 28 and 30, were it was too cloudy all day. Many other days on the transect, especially from May 5 to May 14 and also some days later on, allowed measurements throughout the whole day from sunrise to sunset, performing 10 measurements roughly every 10 minutes with the Microtops units and permanent measurements with FUBISS-ASA2. The two Microtop units agreed well (Figure 5.8.3).

In this time, three major Saharan dust layers were crossed, with maxima of AOD and minima of Angstrom exponent (indicating rather large particles) on May 4, 12, 15 and 22/23 (end of cruise), and pristine conditions before May 1st and between the 6th 8th of May, overall complying well with the predictions of different aerosol distribution models for this region.



FUB (WeW) MICROTOPS II unit 16340 on RV Meteor, GSFC AERONET level 1.5 data, jonas.bismarck@wew.fu-berlin.de

Fig.5.14 Daily averages of the FUB Microtops unit measurements of AOD at 500nm and the Angstrom exponent. The error bars indicate the standard deviation of the values retrieved for each day. The data on day 142 (May 23, RV METEOR in Mindeloharbor) may be influenced by sea spray contamination of the entrance window.

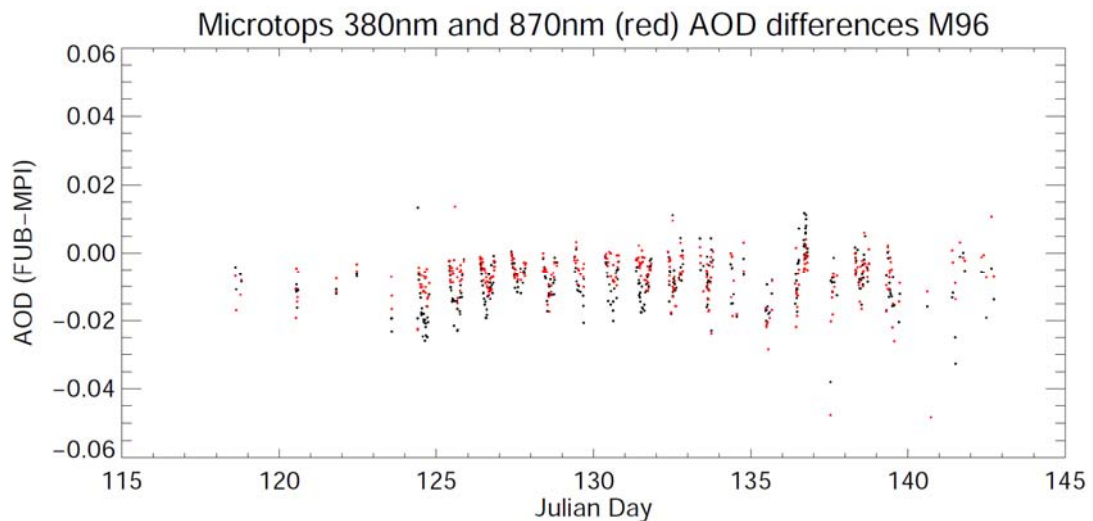


Fig. 5.15 Differences between the AOD values retrieved in the 380nm and 870nm channels of the MPI (operated by Gaby Rädcl and Stefan Kinne/MPI, data processed by Alexander Smirnov/GSFC) and the FUB Microtops units throughout the cruise (derived from GSFC level 1.5 grouped datasets). The uncertainty assumed by GSFC for this type of ship based AOD measurement is 0.02.

Outlook

The further analysis of the data will concentrate on the evaluation of the hyper spectral FUBISS-ASA2 data, including the inversion of particle type classes from the aureole data. The synergy of the combined data recorded during the cruise from the atmosphere remote sensing instruments on board, among others the OCEANET Raman LIDAR and the different Sun photometers, will allow a detailed study of the optical, but also micro-physical properties of the Saharan dust layers passing the vessel on their way from the Sahara to the West. Furthermore, the HATPRO microwave radiometer on the OCEANET container provides accurate measurements of the water vapour column, which can be used to perform a calibration of the channels of FUBISS-ASA2 and the microtops II situated within water vapour absorption bands and thus leading to an enhancement of the quality of the water vapour abundance retrieved with the Sun photometers (Figure 5.16).

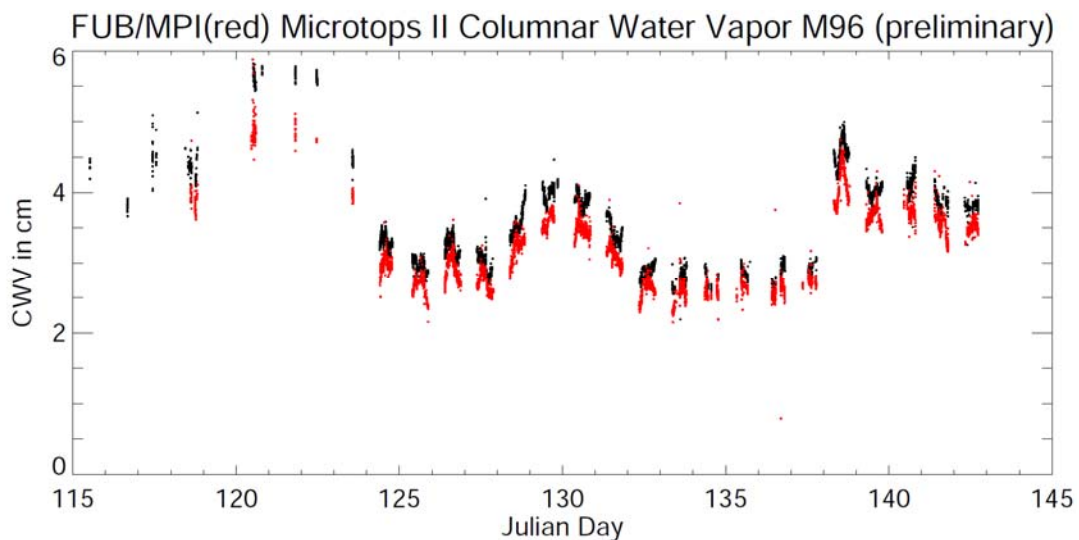


Figure 5.16 Preliminary water vapor product (GSFC level 1.5) of the FUB Microtops II unit (black dots) and the MPI/GSFC Microtops II unit (red dots, for comparison).. This product does not yet include the fine tuning of the retrieval using a measured spectral sensor response function or the OCEANET/HATPRO microwave data.

URMS/AMSSP: Multi-angle measurements of atmospheric and water leaving radiances

Optical remote sensing of the water properties, Aerosol and Clouds in the atmospheric are the main topics of the instrument setup URMS/AMSSP. There are currently large differences between measurements of in-situ and remote sensing methods to derive parameters of water constituents like chlorophyll concentrations and colored dissolved organic matter (CDOM, case one waters). These differences are due to difficulties to modulate the optical properties inside of the water and the assumptions which are made for atmospheric scattering of aerosols and clouds in radiative transfer models. The improvement of the models and to compare the results with different measurement techniques and geometries are the objectives of the cruise on R/V METEOR M96.

URMS (Universal Radiation Measurement System) has the possibility to perform optical multi-directional measurements with different experimental instrument setups. AMSSP

(Airborne Multi-Spectral Sunphoto- &Polarimeter) is the first instrument working with URMS. The AMSSP enables the combined measurement of solar irradiation and polarized radiation. The cruise M96 on the R/V METEOR was the first field deployment and experiment with the system. The measurements will be used as an example and a database to improve the radiation transfer model “MOMO”, which was developed by the Institute of Space Science of FUB. Furthermore we are aiming to improve the understanding and the characterisation of the optical parameter “water leaving radiances” and the impact of parameter changes to the radiation budget of the earth. As an example model simulations show that neglecting the state of polarization of the measured radiances described by the so called “Stokes-vector” and a change in water salinity and temperature can lead to an error of up to $\pm 16\%$ in some spectral regions (Hollstein and Fischer 2012).

URMS/AMSSP was proposed within the framework of the German priority program (PP 1294, Atmosphären- und Erdsystemforschung mit dem Forschungsflugzeug HALO „High Altitude and Long Range Research Aircraft“). The project proposal resulted of the facts that experimental setups with state-of-the-art measurement principles and multi-directional geometries in the field of scientific aircraft radiation measurements are very difficult or not possible to achieve with the existing aircraft and their openings and mounting points. The system can be divided into two parts. A temperature controlled optical container with space for an optical remote sensing instrument and an optical entrance head with a dual mirror system to guide the light into the container. The head can be rotated around two axes to accomplish a wide range of viewing geometries.

The first instrument inside is the Airborne Multispectral Sunphoto- and Polarimeter, which is able to measure the linear stokes vector of the incident light. During the campaign on the R/V METEOR the system was placed on the starboard side on the 4th deck directly at the reeling to provide the best field of view on the ocean and the sky. Since the URMS is a prototype and the campaign M96 is the first time it was used, software optimization had to be done. During the campaign we were able to launch the GPS/IMU system of the URMS to retrieve inertial information, which are essential for direction stabilized measurement on a moving platform. We did integrate the already working single measurement programs of the spectrometers, GPS/IMU and motor control into one main application.

The measurements were started on the May 07, 2013 with the completion of the GPS/IMU system. The data was collected without an automatic scanning mode so far. Therefore rotations around primary and secondary axis were done, while the other axis had a defined angle. During the measurements the attitude and position data of the instrument were recorded by the ships and the instruments Navigation systems.

Rotation axis angles between 10° - 80° towards the horizon were chosen for the primary axis to perform measurements with different measurement geometries. Rotations around the secondary axis were performed in such a way that a plane perpendicular to the horizon was measured. During these “semi-automatic scan” observations of a single spectral measurement the signal integration times did vary between 100 and 5000ms depending on atmospheric conditions and sun elevation. This high dynamic range was anticipated, but made an automatic mode with scanning capability difficult with the available software programs.

Measurement Days and raw data sets during the cruise:*AMSSP:*

AMSSP_20130504 AMSSP_20130507 AMSSP_20130510 AMSSP_20130513
AMSSP_20130516 AMSSP_20130519 AMSSP_20130505 AMSSP_20130508
AMSSP_20130511 AMSSP_20130514 AMSSP_20130517 AMSSP_20130520
AMSSP_20130506 AMSSP_20130509 AMSSP_20130512 AMSSP_20130515
AMSSP_20130518

URMS:

(URMS_20130430, URMS_20130501, URMS20130502, URMS_20130503 testing periode)
URMS_20130505, URMS_20130506, URMS_20130508, URMS_20130510, URMS_20130515,
URMS_20130516, URMS_20130518, URMS_20130519, URMS_20130520

The raw data sets are currently not quality controlled or screened for instrumental or software failures. We will analyze the results after the cruise and in combination with a Master thesis.

5.9 Aerosol, Cloud and raditation measurements: OCEANET

(Ronny Engelmann, Annett Skupin, Alexandra Pietsch)

The OCEANET container is a mobile platform for operation on board of research vessels in order to measure optical properties of aerosols (such as Saharan dust), cloud properties (liquid water), as well as radiation (visible and thermal). Several instruments are combined and can help to identify the effect of aerosols and meteorological conditions on clouds.

A major research aspect during the R/V METEOR M96 expedition was the observation of possible outbreaks of Saharan dust from the African continent. Recent research questions aim at the aging of dust, i.e., sedimentation of large particles, mixing with other aerosols sources (e.g. biomass burning), or coating and processing of dust within clouds.

The OCEANET Team firstly arrived on 26 April 2013 in the harbour of Point-à-Pitre, Guadeloupe. The Container was already placed at the pier where additional equipment from the FU Berlin was unloaded. In the afternoon the container was loaded onto the portside container place on the sterndeck of the R/V METEOR. On 27 and 28 April the measurement equipment was set up. Cloud camera, radiation- and meteorological sensors (COARS system) as well as the microwave radiometer where placed on the container roof and set into operation mode. The Sun photometer was set up on the monkey deck in order to have longer observation periods with free view towards the sun. To derive the energy budget heat flux measurements were also performed using a turbulence measurement system. A sonic anemometer and a fast absorption hygrometer were mounted above the monkey's deck to derive sensible and latent heat fluxes via the inertial dissipation method. Measurements were completed by precipitation measurements using an optical disdrometer. This allows in combination with latent heat flux estimates for the computation of the local fresh water budget, which strongly influences salinity.

On morning of 28 April the vessel left the harbour. Apparently the ships engines induced voltage spikes on the power lines, so that the two UPS in the container rejected the ships direct power net. Thankfully to the electric department, we could supply the containers UPS's with the buffered power grid on board. After that, all the systems worked exceptionally well.

The lidar was set into operation in the evening of 28 April after filling the laser chiller with water and checking the laser beam alignment. On 1 May last adjustments were performed at the

lidar (replacement of a laser mirror, near-range telescope, angle of the polarizers), so that the data can be used with high quality with the beginning of 2 May.

Precipitation measurements show a major precipitation event on the 2nd of May with maximum precipitation rates exceeding 100 mmh^{-1} based on 1 minute measurement intervals. During most of the remaining time only small precipitation rates were recorded.

At the first few days our continuous Sun photometer measurements were disturbed by different shadows of ship parts during the manoeuvres of the mooring work. The sun-tracker system of the photometer was unable to follow these movements. Since we were on the constant easterly course the photometer could aim at the sun and measure the optical thickness of the atmosphere.

Typical daily operations included the cleaning of all optics on the container roof, calibration of CORAS (dark and with light from an integrating sphere), turning of the lidar during high sun elevations at midday for about 3 hours and polarization calibration of the lidar in the evening.

During the first days of the cruise the sky conditions were very clean with only traces of Saharan dust between 500m and 2000m height (Figure 5.17). They were in fact so clean that we could observe a "green flash" during sunset near Guadeloupe. On May 4 and 5 we observed the first occurrence of dust between 700 and 2500 m with an aerosol optical depth of 0.3 at 500 nm. Afterwards the AOD dropped to clean maritime values of 0.08. As R/V METEOR steamed towards east, from 9 May on a continuous increase in AOD was observed up to 0.4 at 15 May. Depending on the dust transport, the AOD remained between 0.25 and 0.5 for the rest of the cruise leg at $14^{\circ}30'N, 20^{\circ}0.5'W$ on 20 May.

On 10 May at 4:46 UTC R/V METEOR turned southwards for a few hours for a co-located measurement with the space lidar Calipso. In this way, the space lidar with high spatial coverage can be compared to a ground lidar with high quality data.

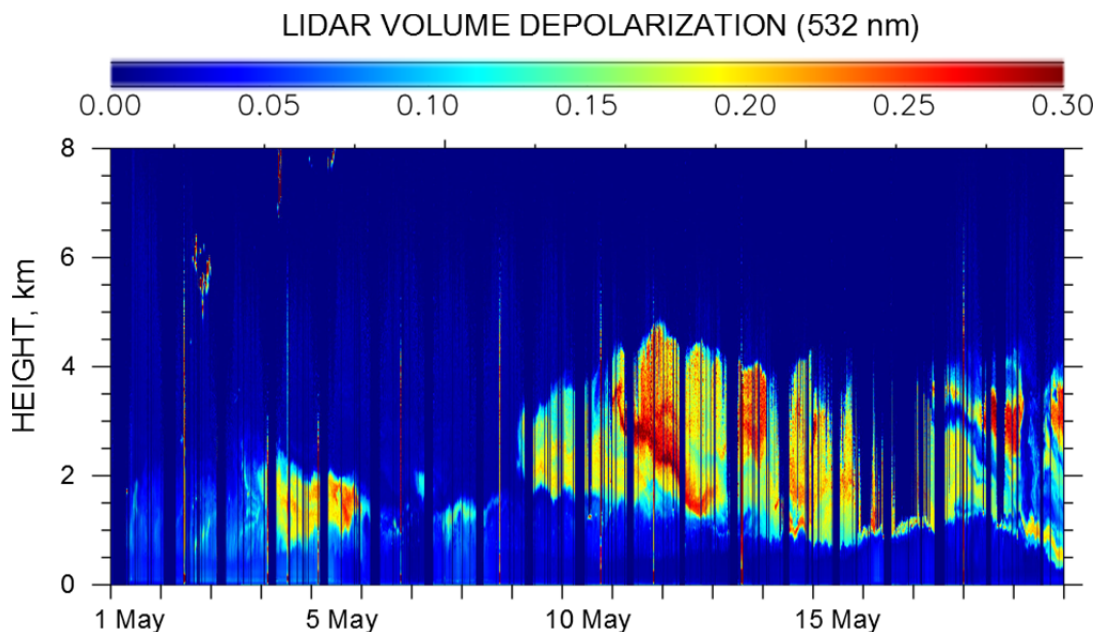


Fig. 5.17. Linear volume depolarization at 532 nm measured with the OCEANET lidar. Values of high depolarization indicate non-spherical particles (Saharan dust) in the atmosphere. The maritime boundary layer (700 - 1000 m height) mostly includes spherical sea salt particles whereas above, up to altitudes of 5 km, dust was observed.

5.10 R/V Meteor and Land based observatories: The Barbados ‘match’

(Stefan Kinne)

Not only a comparison between satellite borne instrumentation and the instrumentation installed on R/V METEOR was done, but also a comparison with a land based observatory on Barbados. In the evening of May 2, the R/V METEOR approached Barbados from the south to about 3 miles of the East Coast of Barbados - directly east of the MPI and NOAA observatories. A CTD profile was acquired (21:34 – 22:19 UTC). The atmospheric observations acquired in the vicinity of Barbados (including observations acquired during the next two days) can be used to compare atmospheric profiles recorded on R/V METEOR with those recorded at the MPI (Deeple Point) and the NOAA (Ragged Point) sites. Two major questions can be answered:

- Is the sampled statistics of clouds (and aerosol) at the (windward) east coast of Barbados representative for the open oceans?
- Over what spatial/temporal scales do low clouds keep their structure?

Radio sonde profiles acquired from the ship showed strongly changing wind-directions and wind-speeds at different altitudes turning from east at the ground to south at 2km and to west and even north-west as well as faster speeds at higher altitudes (in fact the radio sonde, which initially left the ship in a westerly direction must have dropped far off in the easterly direction way ahead of the east moving vessel). The turning wind also explains the northerly wind-shear at the tops of the lower altitude clouds, when looking back towards the MPI site. Over tropical oceans the reversion of wind direction with altitude is also known as Walker circulation.



Fig. 5.18. View back on Barbados, while heading in the 120 degree direction (the wind at the lower cloud base altitude at about 500m). Note the (apparent) island effect, as extra clouds appear over land.

The island effect on cloud cover was easily visible, when leaving the Barbados area and looking back on the island (Figure 5.18). Thus there is the question, if the lower altitude cloud-structures observed at the windward coast capture those of the open ocean. For answers, ship-borne lidar-based times-series of atmospheric profiles of the lower 4 km are compared to data at Barbados offered by a ceilometer (operating at the station same 1024nm wavelength) and by micro pulse lidar (operating at 532nm).

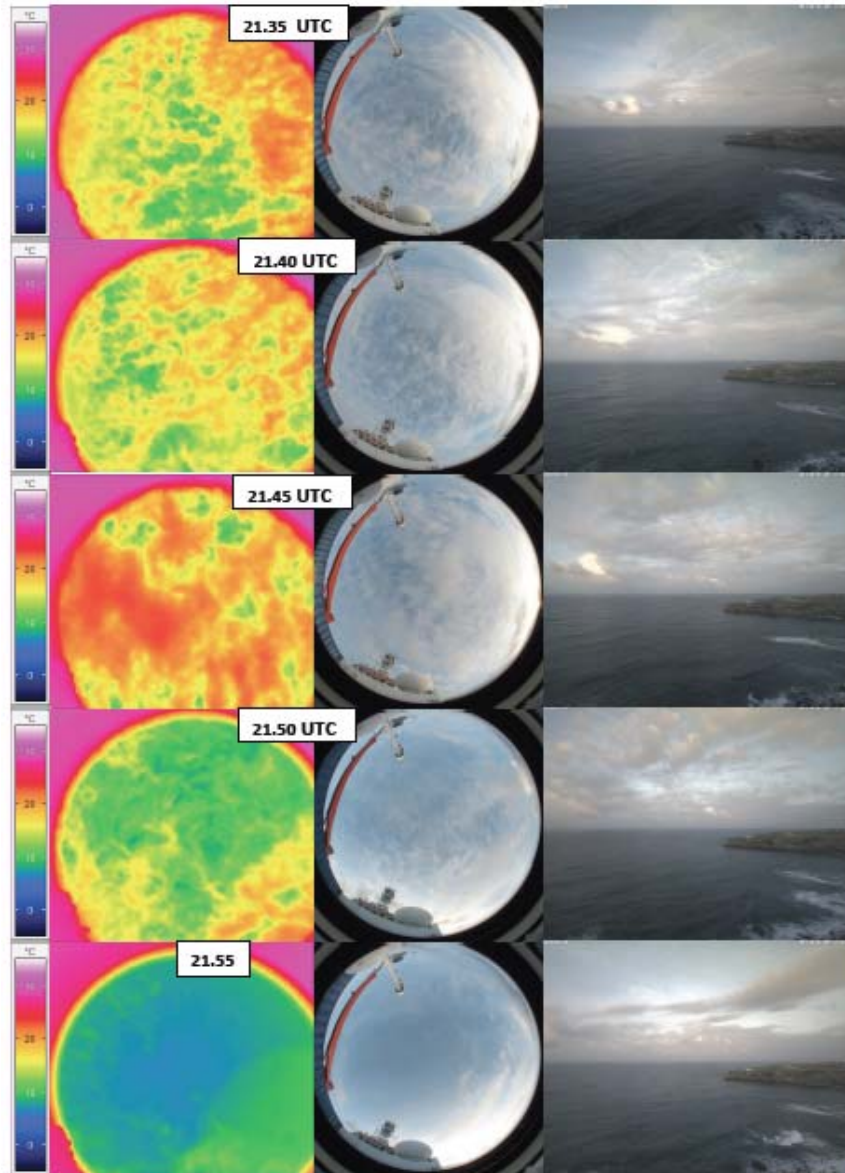


Fig. 5.19 Evening cloud conditions 2 May 2013 off Barbados (IR camera, left; frog cloud-camera, middle; web camera view, right)

Considering the time-period from 21:30 to 22:20 UTC, when the ship was parked 3 miles of the island, intermitted low-cloud cover over the ship was observed (Figure 5.19). Only data samples from the first half of the period are shown, because the second half hardly displayed any low altitude clouds. Hereby, it is apparent, that the images of the (frog-eye) are difficult to imagine, due to the direction distortion, in contrast to the IR camera (~ 30 deg FOV) images or to pictures of the webcam at the MPI site, which is looking towards the ship location. Still, general similarities are encouraging and there should be efforts to combine both data-sets for

investigation of daily cycles for clouds, with daytime images from the cloud camera and night time images from the IR camera. Hereby the temporal aspect (due to generally changing wind-directions with altitude) can be used to identify cloud altitude.

Comparisons of the vertical profile time-series for the 50 minutes, when the R/V METEOR was parked off the observation sites at the coast are presented in Figure 5.20. The focus of this comparison is on patterns for low cloud-structures. These structures are less noisy at 1064nm (of the ceilometer and the ship-lidar) than at 532nm (of the MPL lidar). Hereby the detail of the ship-borne lidar matched neither by the ceilometer nor by the MPL-lidar on land. Still there are similarities, especially between the ceilometer and the ship-lidar above 1km for elevated cloud bases between 1 and 3 km altitude. And even though matches are not perfect (due to the 5km distance in combination with small scale low cloud structures and altitude varying wind-directions and speed) cloud statistics seems similar.

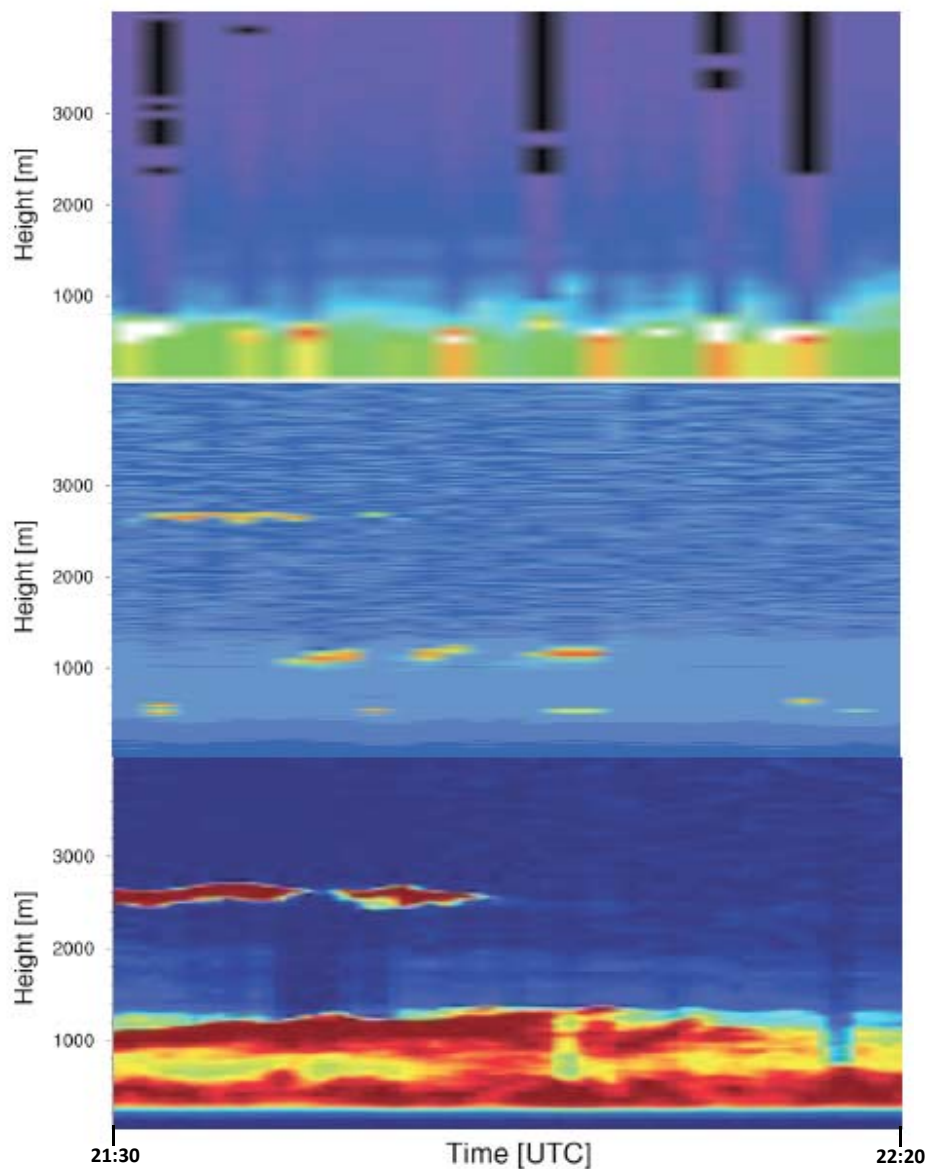


Fig. 5.20 Comparison of vertical profile time-slices for the lower 4 km between the MPL-lidar (532nm, top) and the ceilometer (1064nm, center) and at Barbados and the ship-borne lidar (1064nm, bottom). Period shown is from 21:30 to the 22:20 UTC period on May 2.

To test the spatial extend for such similarities in low cloud patterns (and statistics) the local laser profiles for low cloud bases at Barbados are compared to the complementary ship-borne data, as the vessel moved eastward ($\sim 10\text{km/hr}$) into the wind ($\sim 20\text{km/hr}$). Thus, after adjusting the ship borne times the time-series of profiles for the first 24 hours and for the second 24 hours. We found (not shown here) relatively good agreement in the timing of cloud bases and their altitudes for the first 24h, whereas for the second 24 hours this correlation is lost. This suggests that low level cloud structures have lifetimes that do not exceed one day and that low-cloud structures observed further away than 300 km in distance are largely uncorrelated to local low cloud structures in tropical trade-wind regions. The experiment suggests that (1) the sampled statistics of lowest altitude clouds at the (windward) east coast of Barbados is representative of the statistics over open oceans and (2) over distances of up to 300 km low clouds can keep their structure.

5.11 Microtops Aerosol and Water vapour survey (Gaby Rädcl and Stefan Kinne)

During cloud-free conditions at daytimes, direct solar attenuation samples with handheld Microtops instruments offered data on atmospheric aerosol amount, aerosol size and atmospheric water vapour, offering longitudinal cross sections on these properties.

In collaboration with NASA-GSFC, Microtops measurements are conducted worldwide on an opportunity basis on (research) vessels in order to complement continental aerosol monitoring at AERONET sites. In order to increase the data volume for aerosol reference data over oceans (e.g. for evaluations of satellite retrievals or model simulations) calibrated Microtops instruments are provided along with a GPS unit. The Microtops instrument, when directed towards the sun, captures the solar intensity at five selected sub-spectral solar wavelengths. As with the location and time information of the GPS the incoming solar intensity in these sub-spectral regions at the top of the atmosphere is known, the (smaller) measured value on the ship quantifies the atmospheric attenuation. Since the attenuation can be caused by particles and trace-gases, trace-gas poor sub-spectral regions are selected to attribute the solar attenuation to atmospheric particles. Under cloud-free conditions (thus sun-views contaminated by clouds must be avoided) the attenuation causing particles are aerosol and air molecules. Once the impacts of air-molecules, which are proportional to the surface pressure, are removed, the remaining aerosol attenuation is quantified by the vertically normalized decay exponent, the aerosol optical depth (AOD). With AOD values determined simultaneously at different solar wavelengths, this spectral AOD dependence offers information on aerosol size. Hereby the negative AOD slope with wavelength (in the context of log/log coordinates) is called the Angstrom parameter (AnP). AnP serves as a general indicator for particle size, because larger (super-micron) aerosol particles display little spectral dependence (AnP ~ 0.5 to 0), whereas smaller (sub-micron) aerosol particles have a stronger spectral dependence (AnP ~ 1 to 2). Dust and sea-salt are mainly contributing as super-micron sizes to the AOD, while pollution or wild-fires aerosol mainly contributes to sub-micron AOD. Thus, AnP indirectly offers some insight on aerosol type. In addition to aerosol also atmospheric water vapour is addressed. One of the five solar sub-bands of the Microtops intentionally samples in a band with water vapour absorption, such

that by calculating the difference to a sample without trace-gas absorption (and after vertical normalization) the atmospheric water vapour content can be determined.



Fig. 5.21 Microtops and GPS unit provided by the Marine Aerosol Network of AERONET at NASA-GSFC.

The Microtops measurements are labour-intensive handheld operations, as the instrument (Fig. 5.21) has to be directed towards the position of the sun (hereby the highest transmission signal of 20 measurements within an 8-second sample period is selected in order to eliminate pointing errors). Although these samples are repeated 10 times to identify and exclude by variability the presence of optically thicker and low clouds, these labour intensive measurement methods are rewarded by high quality data with the assurance of cloud-screened data, as visually identified cloud-cases, including especially cases containing high altitude cirrus clouds, are removed as bad samples. The measured Microtops data are transferred via internet to the central NASA location, where the data are available at http://aeronet.gsfc.nasa.gov/new_web/maritime_aerosol_network.html within days.

The latitudinal cross-sections of column properties for aerosol optical depth (AOD), for aerosol Angstrom parameter (AnP) are presented in Figure 5.22, whereas cross-sections for column water vapour and lidar depolarization (an identifier for dust presence provided by the OCEANET lidar), are presented in Figure 5.23. Changes in AOD are associated mainly with variations in dust loading. As dust has a relatively low AnP, days with higher (dust) AOD almost always have a lower AnP. The relatively constant water vapor seems surprising, as the surface and water temperatures have been steadily declining tendency from the western Atlantic to the eastern Atlantic. Interestingly more column water vapor is observed prior to the arrival of larger dust transport events from the Sahara. Complementary lidar data (see Figure 5.17) illustrate that altitudes of relative fresh dust from the Sahara reached altitudes of up to 5 km, whereas aged dust (that had left the Saharan desert more than a week ago) is found only at altitudes up to 3 km.

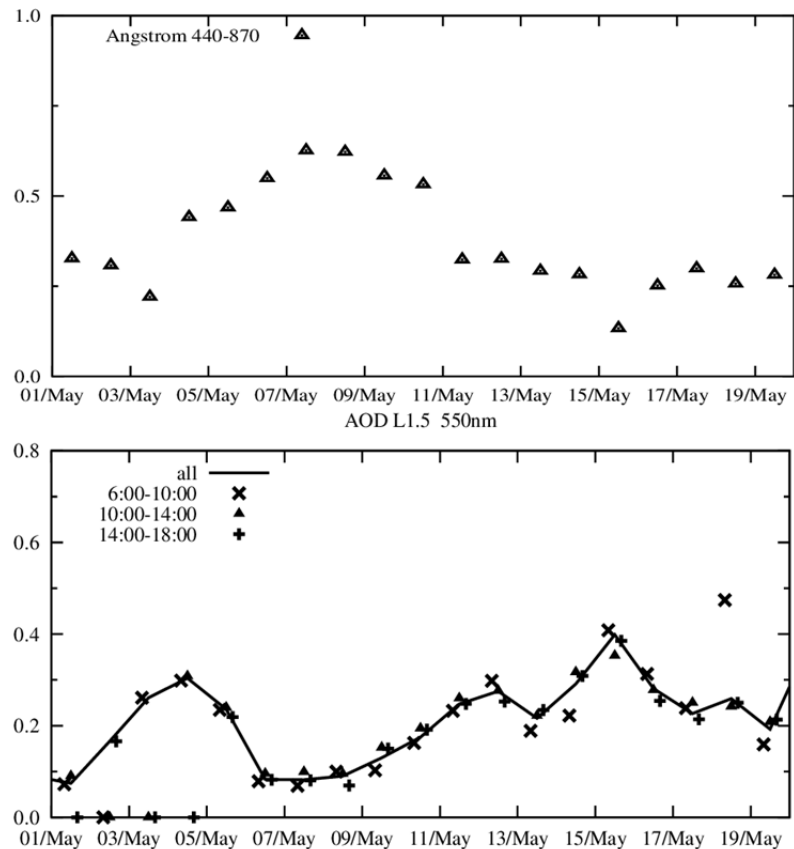


Fig. 5.22 Latitudinal cross-section for atmospheric column properties of AOD at 550 nm (top) and for the Angstrom parameter between 440 and 870 nm (bottom) at 14.5 N in May 2013 across the Atlantic from 60°W to 20°W. Smaller Angstrom parameters indicate the relative stronger presence of larger aerosol size (i.e. dust and sea-salt) and larger Angstrom parameter a relatively stronger presence of smaller aerosol sizes (i.e. from pollution and wildfires): Larger AOD correlate with larger (dust) sizes.

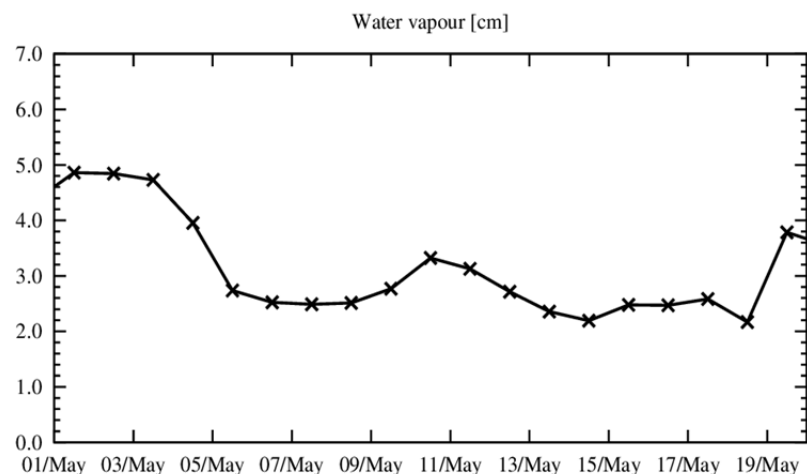


Fig. 5.23 Latitudinal cross-section for atmospheric column properties of water vapor content AOD based on lidar depolarization at 14.5 N in May 2013 across the Atlantic from 60 W (May01) to 20 W (May19) longitude. Water vapor column maxima occur prior to occurrences of larger dust events (May10, May19).

5.12 Particulate matter (>60 μ m) sizing and imaging with the UVP5

(Pieter Vandromme)

The particulate matter distribution within the whole water column was observed through a camera system, the Underwater Video Profiler (UVP5, Picheral et al., 2010), kindly shared by Dr. Lars Stemmann of the Laboratory of Oceanography of Villefranche-sur-Mer, France. The system consists mainly of a “smart cam” (the camera is associated to a computer allowing direct treatments of images within the camera), a 9mm fixed focal lens and 2 lights strobes in front of the camera flashing in the red wavelength (the detailed description of the UVP5 could be found in Picheral et al., 2010). The system was mounted on the CTD/Rosette (Figure 5.24) and profiles the water column during the down cast at a frequency of 11 images per second. One image photographs the content of 0.93L of water, giving, with a CTD/Rosette of about 0.5m/s in the first 100m and 1m/s afterward, an average of 1.86m³ imaged from the surface to 100m depth and an additional 9.3m³ per 1000m of cast.

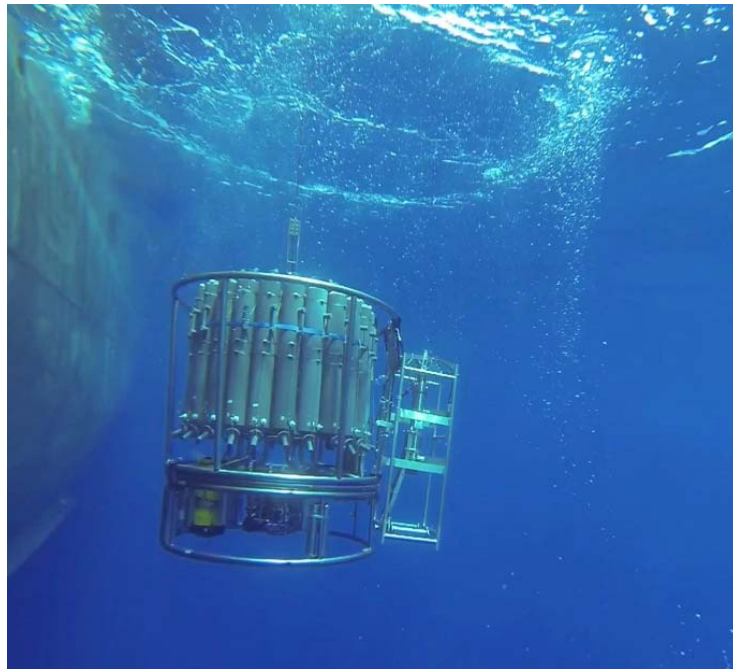


Fig. 5.24 The CTD/Rosette in action during M96 cruise with the UVP5 attached on the right outside of the CTD/Ro.

During the R/V METEORM96 transect a total of 210,205m were imaged in 58 profiles and 1,965,983 images (total of 1828m³ of water). The UVP5 was removed from the CTD/Rosette during the two casts that went deeper than 6000m deep (stations 41 and 45), and technical problems (most probably overheating) provoked a failure in the camera system which didn't worked during three other casts (stations 21, 23 and 39). Following the transect, two “yoyo” stations were made off Cape-Verde on the sunset and on the sunrise. The first “yoyo” consisted of 7 casts performed in a row from the surface to 300m depth from 5pm to 7pm local time. The second “yoyo” consisted of 10 casts in a row from the surface to 300m depth and from 4am to 7am local time. These “yoyos” were performed with the objective to observe the vertical migration of zooplankton at a high temporal resolution. A very last station was performed next to the Cape-Verde Ocean Observatory (CVOO).

The pixel size of images is of $\sim 150 \mu\text{m}$ length, and particles as small as $60 \mu\text{m}$ ESD (Equivalent Spherical Diameter) will excite one pixel and will be counted by the camera (see Picheral et al., 2010, for more explanations). The smart cam allows a direct processing of images within the camera. This process consists of identifying Regions Of Interest (ROI) on images, that is regions with one pixel or with contiguous pixels higher than a certain threshold on the grey scale. In real-time the smart cam provides information on the total number of particles to the CTD via an analogue connection (different settings would have allowed getting real-time information on the sum of the area of ROI per image or on the average grey level). Size and grey level of each ROI is recorded, yet, only images of ROI of at least 33 pixels ($\sim 600 \mu\text{m}$ ESD) are saved by the camera for further identification. A total of 59,107 ROI larger than $600 \mu\text{m}$ ESD were recorded during the transect.

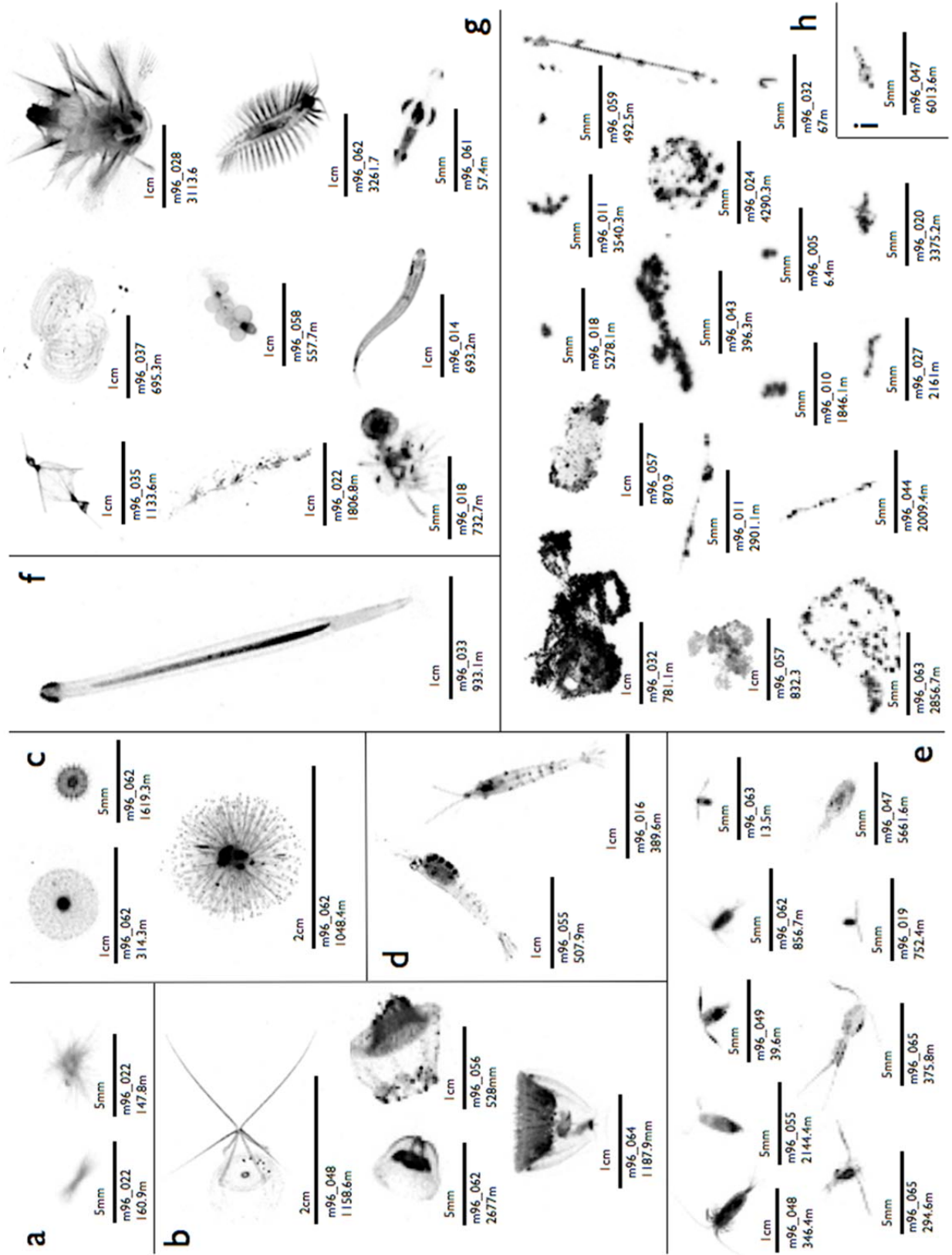


Fig. 5.25 Examples of objects recorded by the UVP5 during the M96 cruise. Below each object the scale, the station number and the depth at which the object was recorded. (a): deep *Trichodesmium* colonies at station 22. (b): jellyfish. (c): radiolarians. (d): shrimp-like. (e): copepods, including the deepest observed at 5661.6 meter depth. (f): chaetognaths. (g): other kind of plankton: appendicularians, siphonophores, fish larvae, annelida... (h): marine snow and other kind of detritus. (i) the deepest object observed during M96 (6013.6m), yet, unidentified

These particles, living and non-living will be sorted afterwards through computer supervised classification and visual validation. This work will be done at the GEOMAR Institute in Kiel by Helena Hauss, Rainer Kiko and Pieter Vandromme helped in this task by students (hiwis). The most common categories in which particles are sorted is shown in Figure 5.25. (Images from M96 cruise).

From the counting and sizing of particles $>60\mu\text{m}$ ESD regardless of the category they belong to many relevant information on the characteristics of the particles community could be extracted (e.g., Guidi et al. 2008). As a first sight, the total number of particles in the water column already gave a nice view of the changes that occurred during the R/V METEOR M96 cruise (Figure 5.26). A maximum of particles reaching concentration of about 60 particles per liter was generally recorded between 100 and 150m depth except on the western side of the transect (Figure 5.26, lower panel).

From $\sim 50^\circ\text{W}$ to Cape-Verde this maximum seems to have increased in strength and to become shallower. Looking at the full depth range (Figure 5.26, upper panel) a strong signal close to Cape-Verde ($\sim 24^\circ\text{W}$) is observed with a concentration of particles from the surface to 4000 m depth always higher than 20 particles per liter and a deep maximum of ~ 35 particles per liter at ~ 2000 m depth.

Except stations close to Cape-Verde, the east side of the transect shows an overall lower deep concentration of particles than the West side. Distribution of particles from ~ 1000 m depth to the bottom is not homogenous with often patches of increased concentration at various depths. Another strong signal of particles concentration is observed close to the sea floor. Particles concentration in the last hundreds meter strongly increased, reaching values of almost 80 particles per liter in the west side of the transect. These bottom maximum were sometimes higher than the sub-surface maximum.

The particles dataset collected during the M96 cruise with the Underwater Video Profiler 5 will greatly contribute to research on the carbon pump on the tropical Atlantic Ocean. Moreover, the image based dataset will provide information on the spatial and vertical distribution of key planktonic groups such as the position during daytime and night time of large copepods or the abundance and exact depth of *Trichodesmium* colonies (diazotrophs filamentous cyanobacteria) in the surface layer.

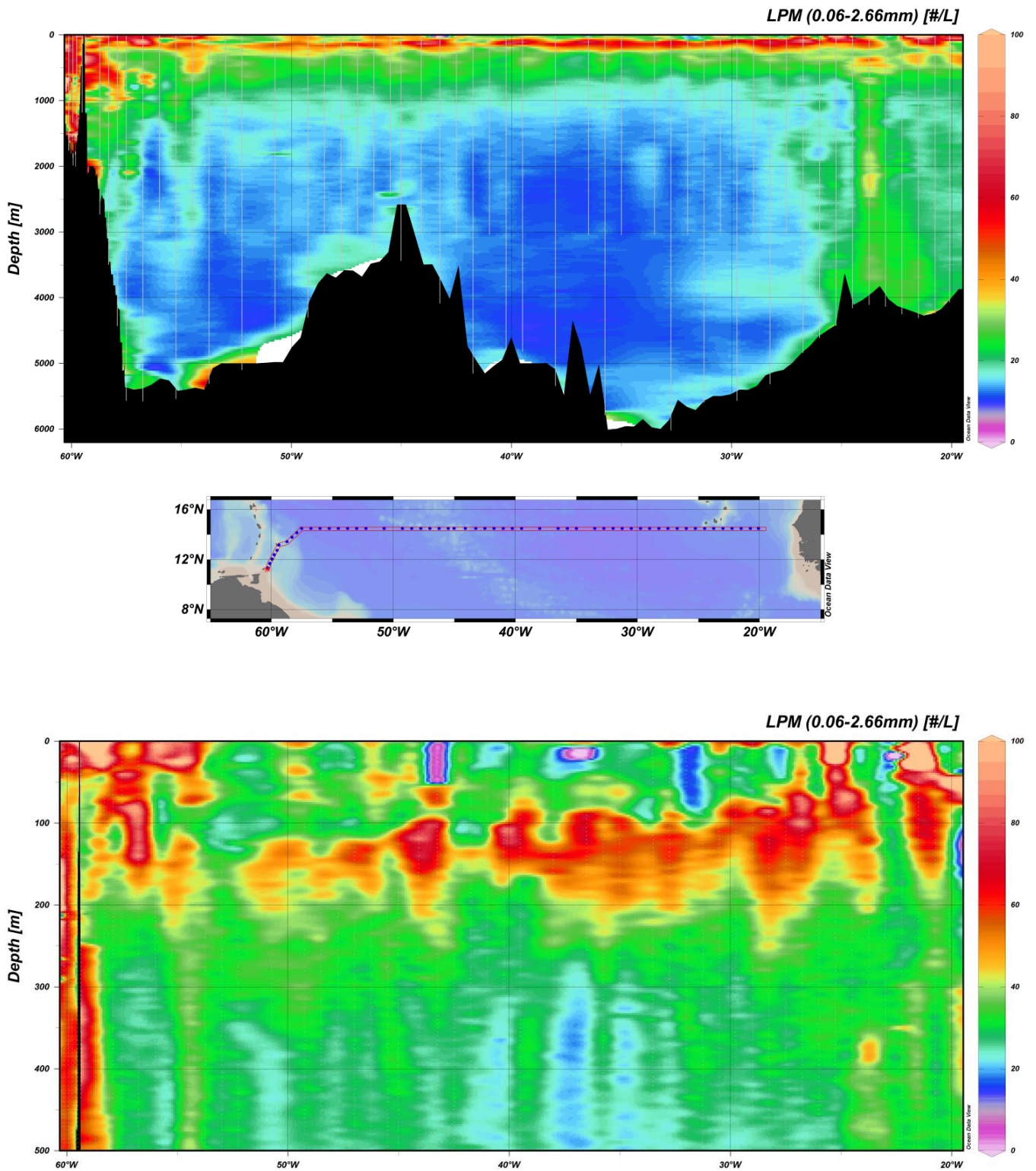


Fig. 5.26 Vertical distribution of particles from 60µm to 2.66 mm ESD during the transect. Upper panel shows the vertical distribution from the surface to 6000 m depth, while the lower panel shows it from the surface to 500 m depth only (different colorscale)

6 Ship's Meteorological Station (Martin Stelzer)

R/V METEOR left the port of Pointe-a-Pitre on 28th of April, 2013 at 12:40 UTC for expedition M96. The research track went along 14°30'N to Mindelo/Cape Verde. When starting the journey the research area of the R/V METEOR was on the southern flank of a high pressure zone over the east coast of the USA, in a region of stable trade winds. The wind blew with 3 to 4 Bft from the east. After leaving protection of land, the significant wave height (combined wind sea and swell) was between 2.5 and 3m, the swell came from easterly directions. Partly heavy rain showers crossed or passed the vessel from time to time. During 28th and 29th of April, R/V METEOR remained on position 16.2°N 60.3°W due to several anchoring and CTD work. The wind blew constantly from the east with 4 Bft. The significant wave height was about 3m. On the evening of 30th of April the transit to the working area, located in the south of Barbados and northeast of Trinidad/Tobago (11.2°N/60.2°W), began. During the transit wind reached 4 to 5 Bft, remaining on easterly direction. The significant wave height was about 3m and decreased to 2 m on way to the south. On the transit the R/V METEOR crossed areas with some heavy rain showers from time to time. On the evening of 01st of May the R/V METEOR reached the working area at 11.2°N, 60.2°W, during a lightning storm. On 02nd and 03rd of May the R/V METEOR went on a northeast course to position 14.3°N 57.3°W. The wind blew from east to southeast with 4 Bft. The significant wave height was about 2 m, the swell was still coming from the east. On the afternoon of 03rd of May, R/V METEOR began her journey along latitude 14.3° N to the east.

An intensifying high pressure area near Newfoundland and Nova Scotia moved slowly south-east to a position near 38N 53W. An associated broad ridge expanded southward to the shipping area of the R/V METEOR R, and became weather effective for the R/V METEOR later this week. From 04th of May the significant wave height decreased slowly to 1m. The south-easterly wind also weakened to 2 to 3 Bft on 5th of May. The just mentioned high pressure area moved further east towards the Azores and with it, the wide ridge. The R/V METEOR went further to the east from 06th until 10th of May, with the high pressure area causing mostly fair conditions. The wind blew constantly from the east with 3 to 4 Bft, the significant wave height was 1 to 1.5 m, and the swell came from a north-easterly direction.

As of 10th of May the wind increased slowly to 4 to 5Bft. On 11th of May wind veered north-east with constant 5Bft. Also the significant wave height increased up to 1.5 -2m.

In the coming days the stable Azores High changed its position only slightly, with the research field of R/V METEOR on its southern flank remaining under the influence of the trade winds.

From 15th of May, the R/V METEOR was now on position 14.3°N 31.1°W, the wind gathered speed again and blew with 5 to 6 Bft from north-easterly directions. But the significant wave height remained at about 2m. Also the north-easterly direction of the swell did not change. On the night from 15th to 16th of May the wind rose to 7Bft for a few hours, but get back to 5-6 Bft for the rest of the night and the next days. On 20th of May the wind decreased and blew temporarily from northerly directions with 3 to 4Bft. The swell came from the North with 1.5 to 2m, the ocean remained relatively quiet due to the weak wind sea. At 8 o'clock, on position 14°30'N 20°07'W, the last CTD lifted out of the water and the R/V METEOR started the transit to Mindelo. On 21st and 22nd of May the wind increased slightly and was blowing from north to

northeast with 4 to 6 Bft. The significant wave height was 2 to 2.5 m, the swell came from the northerly directions. On 22nd of May, 2013, about 19 UTC R/V METEOR reached the port of Mindelo/Cape Verde.

7 Station list

Gear coding

CTD/RO: Conductivity/Temperature/Depth sonde/ lowered Acoustic Doppler Current

Profiler/and rosette sampler

CTD-U: Underway CTD

MOOR: Mooring operation

PIES: Pressure Inverted Echosounders

ISP: in-situ pump

MTEOR Station	Cast	Date	Time	PositionLat	PositionLon	Gear	Action
M960/600-1	MOVE 4-10	4/28/13	19:00	16° 22.16' N	60° 36.83' W	MOR	released
M960/600-1	MOVE 4-10	4/28/13	22:52	16° 22.87' N	60° 37.80' W	MOR	recovered
M960/601-1	CTD 1	4/29/13	1:46	16° 21.28' N	60° 33.47' W	CTD/RO	failed
M960/601-1	CTD 1	4/29/13	2:50	16° 21.28' N	60° 33.47' W	CTD/RO	failed
M960/601-1	CTD 1	4/29/13	4:37	16° 21.30' N	60° 33.45' W	CTD/RO	at depth (1000m)
M960/602-1	CTD 2	4/29/13	7:08	16° 21.42' N	60° 33.30' W	CTD/RO	at depth (3480m)
M960/603-1	MOVE 3-10	4/29/13	9:55	16° 20.34' N	60° 30.65' W	MOR	released
M960/603-1	MOVE 3-10	4/29/13	18:47	16° 21.86' N	60° 32.76' W	MOR	on deck
M960/604-1	Telemetry	4/29/13	20:47	16° 20.30' N	60° 29.36' W	PIES	failed
M960/606-1	in-situ pump 1	4/29/13	23:04	16° 21.58' N	60° 30.26' W	ISP	pump at depth (60m)
M960/605-1	Telemetry	4/29/13	23:28	16° 21.56' N	60° 30.08' W	PIES	failed
M960/606-1	in-situ pump 2	4/30/13	4:19	16° 24.29' N	60° 32.71' W	ISP	pump at depth (60m)
M960/607-1	MOVE 3-11	4/30/13	9:42	16° 23.88' N	60° 40.33' W	MOR	start deployment
M960/607-1	MOVE 3-11	4/30/13	17:42	16° 20.07' N	60° 29.64' W	MOR	weight to water
M960/608-1	MOVE 4-11	4/30/13	19:23	16° 20.92' N	60° 41.61' W	MOR	start deployment
M960/608-1	MOVE 4--11	4/30/13	22:29	16° 19.96' N	60° 36.21' W	MOR	weight to water
M960/609-1	uCTD begin	5/1/13	17:43	12° 58.13' N	60° 7.10' W	CTD-U	
M960/621-1	uCTD end	5/2/13	2:14	11° 22.80' N	60° 17.69' W	CTD-U	
M960/622-1	CTD 3	5/2/13	3:36	11° 20.01' N	60° 17.96' W	CTD/RO	at depth (859m)
M960/623-1	uCTD begin	5/2/13	4:35	11° 24.99' N	60° 15.45' W	CTD-U	
M960/625-1	uCTD end	5/2/13	6:04	11° 40.42' N	60° 7.55' W	CTD-U	
M960/626-1	CTD 4	5/2/13	7:00	11° 41.10' N	60° 7.18' W	CTD/RO	at depth (1744m)
M960/627-1	uCTD begin	5/2/13	8:52	11° 50.05' N	60° 2.62' W	CTD-U	
M960/628-1	uCTD end	5/2/13	9:37	11° 57.86' N	59° 58.63' W	CTD-U	
M960/629-1	CTD 5	5/2/13	10:46	12° 2.23' N	59° 56.46' W	CTD/RO	at depth (1326m)
M960/630-1	uCTD begin	5/2/13	12:04	12° 9.68' N	59° 52.58' W	CTD-U	
M960/631-1	uCTD end	5/2/13	12:57	12° 18.98' N	59° 47.82' W	CTD-U	
M960/632-1	CTD 6	5/2/13	14:00	12° 23.33' N	59° 45.63' W	CTD/RO	at depth (1256m)
M960/633-1	uCTD begin	5/2/13	14:42	12° 24.39' N	59° 44.88' W	CTD-U	
M960/635-1	uCTD end	5/2/13	16:24	12° 39.40' N	59° 34.18' W	CTD-U	
M960/637-1	CTD 7	5/2/13	18:32	12° 44.43' N	59° 30.66' W	CTD/RO	at depth (1200m)

M960/638-1	uCTD begin	5/2/13	19:36	12° 49.10' N	59° 28.92' W	CTD-U	
M960/639-1	uCTD end	5/2/13	20:05	12° 53.96' N	59° 27.12' W	CTD-U	
M960/640-1	CTD 8	5/2/13	22:10	13° 9.78' N	59° 22.92' W	CTD/RO	at depth (442m)
M960/641-1	uCTD begin	5/2/13	23:06	13° 7.11' N	59° 16.81' W	CTD-U	
M960/648-1	uCTD end	5/3/13	2:29	13° 22.71' N	58° 48.63' W	CTD-U	
M960/649-1	CTD 9	5/3/13	4:12	13° 26.59' N	58° 42.62' W	CTD/RO	at depth (2704m)
M960/650-1	CTD 10	5/3/13	9:35	13° 47.77' N	58° 18.60' W	CTD/RO	at depth (3419m)
M960/651-1	uCTD begin	5/3/13	11:28	13° 51.32' N	58° 14.57' W	CTD-U	
M960/653-1	uCTD end	5/3/13	13:20	14° 5.56' N	57° 58.38' W	CTD-U	
M960/654-1	CTD 11	5/3/13	15:46	14° 8.88' N	57° 54.60' W	CTD/RO	at depth (4386m)
M960/655-1	uCTD begin	5/3/13	17:45	14° 12.90' N	57° 50.04' W	CTD-U	
M960/659-1	uCTD end	5/3/13	19:25	14° 26.25' N	57° 34.87' W	CTD-U	
M960/660-1	CTD 12	5/3/13	21:44	14° 30.00' N	57° 30.60' W	CTD/RO	at depth (5478m)
M960/661-1	uCTD begin	5/4/13	1:06	14° 30.00' N	57° 23.07' W	CTD-U	
M960/669-1	uCTD end	5/4/13	3:39	14° 30.00' N	56° 52.74' W	CTD-U	
M960/670-1	CTD 13	5/4/13	6:26	14° 30.00' N	56° 45.00' W	CTD/RO	at depth (5487m)
M960/671-1	uCTD begin	5/4/13	9:20	14° 30.00' N	56° 30.40' W	CTD-U	
M960/679-1	uCTD end	5/4/13	11:42	14° 30.03' N	56° 2.31' W	CTD-U	
M960/680-1	CTD 14	5/4/13	12:24	14° 30.00' N	56° 0.00' W	CTD/RO	at depth (981m)
M960/681-1	CTD 15	5/4/13	14:34	14° 30.00' N	56° 0.00' W	CTD/RO	at depth (2996m)
M960/682-1	uCTD begin	5/4/13	16:43	14° 30.00' N	55° 53.63' W	CTD-U	
M960/691-1	uCTD end	5/4/13	19:30	14° 30.00' N	55° 20.71' W	CTD-U	
M960/692-1	CTD 16	5/4/13	21:45	14° 30.01' N	55° 15.01' W	CTD/RO	at depth (5448m)
M960/693-1	uCTD begin	5/5/13	0:50	14° 30.00' N	55° 4.60' W	CTD-U	
M960/700-1	uCTD end	5/5/13	2:54	14° 30.00' N	54° 40.09' W	CTD-U	
M960/701-1	CTD 17	5/5/13	4:54	14° 29.98' N	54° 29.99' W	CTD/RO	at depth (3327m)
M960/702-1	uCTD begin	5/5/13	6:44	14° 30.00' N	54° 23.49' W	CTD-U	
M960/711-1	uCTD end	5/5/13	9:43	14° 30.00' N	53° 47.55' W	CTD-U	
M960/712-1	CTD 18	5/5/13	11:39	14° 30.00' N	53° 45.00' W	CTD/RO	at depth (5227m)
M960/713-1	uCTD begin	5/5/13	14:06	14° 30.00' N	53° 37.89' W	CTD-U	
M960/721-1	uCTD end	5/5/13	16:40	14° 30.00' N	53° 7.11' W	CTD-U	
M960/722-1	CTD 19	5/5/13	18:21	14° 30.00' N	53° 0.01' W	CTD/RO	at depth (3000m)
M960/723-1	uCTD begin	5/5/13	20:21	14° 30.00' N	52° 47.30' W	CTD-U	
M960/727-1	uCTD end	5/5/13	22:42	14° 30.00' N	52° 19.48' W	CTD-U	
M960/728-1	CTD 20	5/6/13	0:47	14° 29.99' N	52° 15.02' W	CTD/RO	at depth (5019m)
M960/729-1	uCTD begin	5/6/13	3:02	14° 35.60' N	52° 10.63' W	CTD-U	
M960/738-1	uCTD end	5/6/13	7:49	15° 21.19' N	51° 35.05' W	CTD-U	
M960/739-1	MOVE 1-10	5/6/13	8:53	15° 27.06' N	51° 30.77' W	MOR	
M960/739-1	MOVE 1-10	5/6/13	12:57	15° 27.31' N	51° 31.77' W	MOR	Recovered
M960/740-1	Telemetry	5/6/13	14:07	15° 27.00' N	51° 31.65' W	PIES	Failed
M960/741-1	MOVE 1-11	5/6/13	15:59	15° 30.22' N	51° 39.55' W	MOR	deployment
M960/741-1	MOVE 1-11	5/6/13	21:35	15° 26.77' N	51° 29.88' W	MOR	deployment
M960/742-1	CTD 21	5/7/13	0:14	15° 26.11' N	51° 29.77' W	CTD/RO	at depth (4945m)
M960/743-1	in-situ pump 3	5/7/13	2:12	15° 26.11' N	51° 29.77' W	ISP	pump at depth (70m)
M960/744-1	uCTD begin	5/7/13	3:02	15° 26.11' N	51° 29.77' W	CTD-U	
M960/754-1	uCTD end	5/7/13	12:34	14° 32.72' N	50° 47.18' W	CTD-U	
M960/755-1	CTD 22	5/7/13	14:37	14° 30.00' N	50° 45.00' W	CTD/RO	at depth (4508m)
M960/756-1	uCTD begin	5/7/13	17:22	14° 30.00' N	50° 31.06' W	CTD-U	
M960/761-1	uCTD end	5/7/13	19:58	14° 30.00' N	50° 1.32' W	CTD-U	

M960/762-1	CTD 23	5/7/13	21:18	14° 30.00' N	50° 0.00' W	CTD/RO	at depth (3007m)
M960/763-1	uCTD begin	5/7/13	23:19	14° 30.00' N	49° 52.00' W	CTD-U	
M960/768-1	uCTD end	5/8/13	2:06	14° 30.00' N	49° 21.55' W	CTD-U	
M960/769-1	CTD 24	5/8/13	4:11	14° 30.01' N	49° 15.02' W	CTD/RO	at depth (4241m)
M960/770-1	uCTD begin	5/8/13	6:16	14° 30.00' N	49° 9.41' W	CTD-U	
M960/776-1	uCTD end	5/8/13	9:26	14° 30.00' N	48° 33.02' W	CTD-U	
M960/777-1	CTD 25	5/8/13	10:48	14° 30.03' N	48° 30.01' W	CTD/RO	at depth (3006m)
M960/778-1	uCTD begin	5/8/13	12:33	14° 30.00' N	48° 23.41' W	CTD-U	
M960/784-1	uCTD end	5/8/13	15:31	14° 30.00' N	47° 48.89' W	CTD-U	
M960/785-1	CTD 26	5/8/13	17:05	14° 30.00' N	47° 45.01' W	CTD/RO	at depth (3489m)
M960/786-1	uCTD begin	5/8/13	18:38	14° 30.00' N	47° 40.08' W	CTD-U	
M960/792-1	uCTD end	5/8/13	21:41	14° 30.00' N	47° 5.07' W	CTD-U	
M960/793-1	CTD 27	5/8/13	23:13	14° 30.00' N	47° 0.01' W	CTD/RO	at depth (3006m)
M960/794-1	uCTD begin	5/9/13	1:03	14° 30.00' N	46° 50.80' W	CTD-U	
M960/799-1	uCTD end	5/9/13	3:38	14° 30.00' N	46° 20.72' W	CTD-U	
M960/800-1	CTD 28	5/9/13	5:16	14° 30.00' N	46° 15.00' W	CTD/RO	at depth (3296m)
M960/801-1	uCTD begin	5/9/13	7:08	14° 30.00' N	46° 7.38' W	CTD-U	
M960/807-1	uCTD end	5/9/13	10:10	14° 30.00' N	45° 32.08' W	CTD-U	
M960/808-1	CTD 29	5/9/13	11:22	14° 30.00' N	45° 30.01' W	CTD/RO	at depth (2402m)
M960/809-1	uCTD begin	5/9/13	12:37	14° 30.00' N	45° 25.62' W	CTD-U	
M960/813-1	uCTD end	5/9/13	14:19	14° 30.00' N	45° 5.26' W	CTD-U	
M960/814-1	CTD 30	5/9/13	15:54	14° 30.00' N	45° 1.23' W	CTD/RO	at depth (3397m)
M960/815-1	uCTD begin	5/9/13	17:50	14° 30.00' N	44° 52.15' W	CTD-U	
M960/822-1	uCTD end	5/9/13	21:25	14° 30.00' N	44° 9.50' W	CTD-U	
M960/823-1	CTD 31	5/9/13	22:51	14° 29.99' N	44° 6.00' W	CTD/RO	at depth (3006m)
M960/824-1	uCTD begin	5/10/13	6:32	14° 30.00' N	43° 59.35' W	CTD-U	
M960/829-1	uCTD end	5/10/13	9:40	14° 30.00' N	43° 23.49' W	CTD-U	
M960/830-1	CTD 32	5/10/13	11:46	14° 30.02' N	43° 15.01' W	CTD/RO	at depth (4034m)
M960/831-1	uCTD begin	5/10/13	13:33	14° 30.00' N	43° 11.54' W	CTD-U	
M960/838-1	uCTD end	5/10/13	17:11	14° 30.00' N	42° 31.32' W	CTD-U	
M960/839-1	CTD33	5/10/13	18:26	14° 30.00' N	42° 30.00' W	CTD/RO	at depth (3002m)
M960/840-1	uCTD begin	5/10/13	20:54	14° 30.00' N	42° 24.56' W	CTD-U	
M960/846-1	uCTD end	5/11/13	0:03	14° 30.00' N	41° 48.01' W	CTD-U	
M960/847-1	CTD 34	5/11/13	2:15	14° 30.01' N	41° 45.02' W	CTD/RO	at depth (5072m)
M960/848-1	uCTD begin	5/11/13	5:25	14° 30.00' N	41° 37.01' W	CTD-U	
M960/854-1	uCTD end	5/11/13	8:10	14° 30.00' N	41° 5.70' W	CTD-U	
M960/855-1	CTD 35	5/11/13	9:42	14° 30.00' N	41° 0.00' W	CTD/RO	at depth (3008m)
M960/856-1	uCTD begin	5/11/13	11:31	14° 30.00' N	40° 54.44' W	CTD-U	
M960/862-1	uCTD end	5/11/13	14:37	14° 30.00' N	40° 19.84' W	CTD-U	
M960/863-1	CTD 36	5/11/13	16:49	14° 29.99' N	40° 15.01' W	CTD/RO	at depth (4725m)
M960/864-1	uCTD begin	5/11/13	18:45	14° 30.00' N	40° 11.20' W	CTD-U	
M960/870-1	uCTD end	5/11/13	22:05	14° 30.00' N	39° 33.42' W	CTD-U	
M960/871-1	CTD 37	5/11/13	22:55	14° 30.00' N	39° 30.01' W	CTD/RO	at depth (992m)
M960/872-1	CTD 38	5/12/13	1:42	14° 30.00' N	39° 30.01' W	CTD/RO	at depth (5203m)
M960/873-1	uCTD begin	5/12/13	3:58	14° 30.00' N	39° 24.37' W	CTD-U	
M960/879-1	uCTD end	5/12/13	6:52	14° 30.00' N	38° 52.42' W	CTD-U	
M960/880-1	CTD 39	5/12/13	9:24	14° 30.00' N	38° 45.00' W	CTD/RO	at depth (4902m)
M960/881-1	uCTD begin	5/12/13	12:05	14° 30.00' N	38° 35.71' W	CTD-U	
M960/886-1	uCTD end	5/12/13	14:51	14° 30.00' N	38° 5.25' W	CTD-U	

M960/887-1	CTD 40	5/12/13	17:12	14° 30,01' N	38° 0,01' W	CTD/RO	at depth (5260m)
M960/888-1	uCTD begin	5/12/13	19:59	14° 30,00' N	37° 56,48' W	CTD-U	
M960/894-1	uCTD end	5/13/13	2:15	14° 30,00' N	37° 21,12' W	CTD-U	
M960/895-1	CTD 41	5/13/13	4:14	14° 30,00' N	37° 19,78' W	CTD/RO	at depth (6199m)
M960/896-1	uCTD begin	5/13/13	6:41	14° 30,00' N	37° 15,14' W	CTD-U	
M960/904-1	uCTD end	5/13/13	10:32	14° 30,00' N	36° 33,94' W	CTD-U	
M960/905-1	CTD 42	5/13/13	12:00	14° 30,00' N	36° 30,00' W	CTD/RO	at depth (3000m)
M960/906-1	uCTD begin	5/13/13	13:20	14° 30,00' N	36° 26,78' W	CTD-U	
M960/912-1	uCTD end	5/13/13	16:40	14° 30,00' N	35° 49,36' W	CTD-U	
M960/913-1	CTD 43	5/13/13	19:03	14° 30,00' N	35° 45,01' W	CTD/RO	at depth (5675m)
M960/914-1	uCTD begin	5/13/13	21:08	14° 30,00' N	35° 41,45' W	CTD-U	
M960/919-1	uCTD end	5/14/13	0:08	14° 30,00' N	35° 7,59' W	CTD-U	
M960/920-1	CTD 44	5/14/13	1:52	14° 30,00' N	35° 0,01' W	CTD/RO	at depth (3001m)
M960/921-1	uCTD begin	5/14/13	3:34	14° 30,00' N	34° 54,44' W	CTD-U	
M960/927-1	uCTD end	5/14/13	6:18	14° 30,00' N	34° 25,09' W	CTD-U	
M960/928-1	CTD 45	5/14/13	8:28	14° 29,99' N	34° 22,20' W	CTD/RO	at depth (6246m)
M960/929-1	uCTD begin	5/14/13	10:59	14° 30,00' N	34° 16,66' W	CTD-U	
M960/936-1	uCTD end	5/14/13	15:05	14° 30,00' N	33° 32,26' W	CTD-U	
M960/937-1	CTD 46	5/14/13	16:32	14° 30,00' N	33° 30,02' W	CTD/RO	at depth (3007m)
M960/938-1	uCTD begin	5/14/13	18:26	14° 30,00' N	33° 22,62' W	CTD-U	
M960/944-1	uCTD end	5/14/13	21:39	14° 30,00' N	32° 47,80' W	CTD-U	
M960/945-1	CTD 47	5/14/13	23:45	14° 30,00' N	32° 45,01' W	CTD/RO	at depth (6021m)
M960/946-1	uCTD begin	5/15/13	2:16	14° 30,00' N	32° 39,72' W	CTD-U	
M960/953-1	uCTD end	5/15/13	5:28	14° 30,00' N	32° 4,46' W	CTD-U	
M960/954-1	CTD 48	5/15/13	6:59	14° 30,00' N	32° 0,01' W	CTD/RO	at depth (3008m)
M960/955-1	uCTD begin	5/15/13	8:59	14° 30,00' N	31° 55,30' W	CTD-U	
M960/961-1	uCTD end	5/15/13	12:14	14° 30,00' N	31° 20,24' W	CTD-U	
M960/962-1	CTD 49	5/15/13	14:37	14° 30,00' N	31° 15,01' W	CTD/RO	at depth (5498m)
M960/963-1	uCTD begin	5/15/13	17:08	14° 30,00' N	31° 9,60' W	CTD-U	
M960/969-1	uCTD end	5/15/13	20:27	14° 30,00' N	30° 34,12' W	CTD-U	
M960/970-1	CTD 50	5/15/13	21:55	14° 30,00' N	30° 30,00' W	CTD/RO	at depth (3004m)
M960/971-1	uCTD begin	5/15/13	23:37	14° 30,00' N	30° 24,53' W	CTD-U	
M960/977-1	uCTD end	5/16/13	2:52	14° 30,00' N	29° 49,51' W	CTD-U	
M960/978-1	in-situ pump 4	5/16/13	3:27	14° 30,00' N	29° 45,00' W	ISP	pump at depth (85m)
M960/979-1	CTD 51	5/16/13	10:03	14° 30,00' N	29° 45,00' W	CTD/RO	at depth (5473m)
M960/980-1	uCTD begin	5/16/13	12:32	14° 30,00' N	29° 39,57' W	CTD-U	
M960/984-1	uCTD end	5/16/13	15:10	14° 30,00' N	29° 10,24' W	CTD-U	
M960/985-1	CTD 52	5/16/13	17:14	14° 30,00' N	29° 0,00' W	CTD/RO	at depth (3007m)
M960/986-1	uCTD begin	5/16/13	19:19	14° 30,00' N	28° 52,11' W	CTD-U	
M960/989-1	uCTD end	5/16/13	21:03	14° 30,00' N	28° 32,83' W	CTD-U	
M960/990-1	CTD 53	5/17/13	0:18	14° 30,00' N	28° 15,00' W	CTD/RO	at depth (5227m)
M960/991-1	uCTD begin	5/17/13	2:33	14° 30,00' N	28° 9,73' W	CTD-U	
M960/997-1	uCTD end	5/17/13	5:28	14° 30,00' N	27° 35,52' W	CTD-U	
M960/998-1	CTD 54	5/17/13	7:34	14° 29,99' N	27° 30,01' W	CTD/RO	at depth (3006m)
M960/999-1	uCTD begin	5/17/13	9:16	14° 30,00' N	27° 24,27' W	CTD-U	
M960/1003-1	uCTD end	5/17/13	11:57	14° 30,00' N	26° 52,44' W	CTD-U	
M960/1004-1	CTD 55	5/17/13	14:11	14° 29,99' N	26° 45,02' W	CTD/RO	at depth (4768m)
M960/1005-1	uCTD begin	5/17/13	16:32	14° 30,00' N	26° 39,41' W	CTD-U	
M960/1011-1	uCTD end	5/17/13	19:42	14° 30,00' N	26° 4,96' W	CTD-U	

M960/1012-1	CTD 56	5/17/13	21:41	14° 30.00' N	26° 0.00' W	CTD/RO	at depth (4548m)
M960/1013-1	uCTD begin	5/17/13	23:53	14° 30.00' N	25° 55.12' W	CTD-U	
M960/1019-1	uCTD end	5/18/13	2:47	14° 30.00' N	25° 22.40' W	CTD-U	
M960/1020-1	CTD 57	5/18/13	4:55	14° 29.99' N	25° 15.00' W	CTD/RO	at depth (4366m)
M960/1021-1	uCTD begin	5/18/13	7:21	14° 30.00' N	25° 9.57' W	CTD-U	
M960/1025-1	uCTD end	5/18/13	9:43	14° 30.00' N	24° 40.81' W	CTD-U	
M960/1026-1	CTD 58	5/18/13	12:02	14° 30.00' N	24° 30.00' W	CTD/RO	at depth (4103m)
M960/1027-1	uCTD begin	5/18/13	15:05	14° 30.00' N	24° 14.69' W	CTD-U	
M960/1032-1	uCTD end	5/18/13	17:43	14° 30.00' N	23° 46.80' W	CTD-U	
M960/1033-1	in-situ pump 5	5/18/13	18:07	14° 29.98' N	23° 45.02' W	ISP	pump at depth (70m)
M960/1034-1	CTD 59	5/19/13	1:50	14° 30.00' N	23° 45.00' W	CTD/RO	at depth (4055m)
M960/1035-1	uCTD begin	5/19/13	4:09	14° 30.00' N	23° 37.70' W	CTD-U	
M960/1039-1	uCTD end	5/19/13	6:34	14° 30.00' N	23° 7.53' W	CTD-U	
M960/1040-1	CTD 60	5/19/13	8:50	14° 29.99' N	23° 0.00' W	CTD/RO	at depth (4077m)
M960/1041-1	uCTD begin	5/19/13	10:55	14° 30.00' N	22° 51.49' W	CTD-U	
M960/1046-1	uCTD end	5/19/13	13:48	14° 30.00' N	22° 17.73' W	CTD-U	
M960/1047-1	CTD 61	5/19/13	15:36	14° 30.01' N	22° 15.02' W	CTD/RO	at depth (4190m)
M960/1048-1	uCTD begin	5/19/13	18:08	14° 30.00' N	22° 6.05' W	CTD-U	
M960/1053-1	uCTD end	5/19/13	20:55	14° 30.00' N	21° 35.13' W	CTD-U	
M960/1054-1	CTD 62	5/19/13	22:54	14° 30.00' N	21° 30.00' W	CTD/RO	at depth (4251m)
M960/1055-1	uCTD begin	5/20/13	1:06	14° 30.00' N	21° 23.36' W	CTD-U	
M960/1060-1	uCTD end	5/20/13	3:54	14° 30.00' N	20° 50.20' W	CTD-U	
M960/1061-1	CTD 63	5/20/13	5:44	14° 30.00' N	20° 44.99' W	CTD/RO	at depth (4184m)
M960/1062-1	uCTD begin	5/20/13	8:17	14° 30.00' N	20° 39.71' W	CTD-U	
M960/1066-1	uCTD end	5/20/13	10:33	14° 30.00' N	20° 12.56' W	CTD-U	
M960/1067-1	CTD 64	5/20/13	12:34	14° 29.98' N	20° 5.00' W	CTD/RO	at depth (4015m)
M960/1068-1	uCTD begin	5/21/13	7:16	15° 31.34' N	23° 17.44' W	CTD-U	
M960/1083-1	uCTD end	5/21/13	14:52	16° 17.54' N	24° 9.56' W	CTD-U	
M960/1084-1	CTD 65	5/21/13	18:22	16° 34.62' N	24° 29.64' W	CTD/RO	at depth (536m)
M960/1085-1	CTD 66	5/22/13	5:18	17° 42.05' N	24° 42.12' W	CTD/RO	at depth (309m)
M960/1086-1	CTD 67	5/22/13	11:41	17° 34.99' N	24° 17.01' W	CTD/RO	at depth (3578m)

8 Data and Sample Storage and Availability

The Kiel Data Management Team (KDMT) provides an information and data archival system where metadata of the onboard DSHIP-System is collected and publicly available. This Ocean Science Information System (OSIS-Kiel) is accessible for all project participants and can be used to share and edit field information and to provide scientific data, as they become available. The central system OSIS is providing information on granted ship time with information on the scientific program and the general details down to the availability of data files from already concluded cruises. The transparency on the research activities is regarded as an invitation to external scientists to start communication on collaboration on behalf of the newly available data.

The KDMT will take care as data curators to fulfil the here proposed data publication of the data in a World Data Center (e.g. PANGAEA) which will then provide long-term archival and access to the data. The data publication process will be based on the available files in OSIS and is therefore transparent to all reviewers and scientists. This cooperation with a world data center

will make the data globally searchable, and links to the data owners will provide points of contact to project-external scientists. Availability of metadata in OSIS-Kiel (portal.geomar.de/osis): 2 weeks after the cruise. Availability of data in OSIS-Kiel (portal.geomar.de/osis): 6 months after the cruise. Availability of data in a WDC/PANGAEA (www.pangaea.de): 3 years after the cruise.

MOVE mooring data: MOVE is part of the international OceanSITES project (www.oceansites.org), and the data are generally freely available online. OceanSITES maintains two mirrored FTP servers to distribute the data. Pending final processing and QC, the MOVE mooring data obtained during R/V METEOR expedition 96 will be posted to these servers; it is anticipated that this will occur in summer 2013. Permanent archival of OceanSITES data is presently being developed at a NOAA facility in the USA (NODC, National Oceanographic Data Center).

9 Acknowledgements

We like to thank captain Michael Schneider, his officers and crew of R/V METEOR for their support of our measurement program and for creating a very friendly and professional work atmosphere on board. The ship time of R/V METEOR was provided by the German Science Foundation (DFG) within the core program METEOR/MERIAN. Financial support for the different projects carried out during the cruise was provided through the COST Action 1001 (SMOS-MODE), the FP7 GROOM project (GA 284321), and the US National Oceanic and Atmospheric Administration (NOAA; project MOVE).

10 References

During the cruise we followed the guide lines recently developed by the GO-SHIP group, particularly did we consider the guides for best practices:

Hood, E.M., C.L. Sabine, and B.M. Sloyan, eds. 2010. The GO-SHIP Repeat Hydrography Manual: A Collection of Expert Reports and Guidelines. IOCCP Report Number 14, ICPO Publication Series Number 134. Available online at <http://www.go-ship.org/HydroMan.html>.

Specific sections referred to:

Langdon, C. "Determination of Dissolved Oxygen in Seawater by Winkler Titration Using the Amperometric Technique."

Thurnherr, A.M., M. Visbeck, E. Firing, B.A. King, J.M. Hummon, G. Krahnemann, and B. Huber, "A Manual for Acquiring Lowered Doppler Current Profiler Data"

Other literature:

- Baker AR, Weston K, Kelly SD, Voss M, Streu P, Cape JN (2007) Dry and wet deposition of nutrients from the tropical Atlantic atmosphere: Links to primary productivity and nitrogen fixation. *Deep-Sea Res Pt I* 54: 1704-1720.
- Mills MM, Ridame C, Davey M, LaRoche J, Geider RJ (2004) Iron and phosphorus co-limit nitrogen fixation in the eastern tropical North Atlantic. *Nature* 429: 292-294.
- Kanzow, T., Send, U., Zenk, W., Chave, A. and Rhein, M. (2006) Monitoring the integrated deep meridional flow in the tropical North Atlantic: Long-term performance of a geostrophic array *Deep-Sea Research Part I-Oceanographic Research Papers*, 53 (3). pp. 528-546. DOI 10.1016/j.dsr.2005.12.007.
- Send, U., Lankhorst, M. and Kanzow, T. (2011) Observation of decadal change in the Atlantic meridional overturning circulation using 10 years of continuous transport data *Geophysical Research Letters*, 38 (24). DOI 10.1029/2011GL049801.
- Visbeck, M., Deep velocity profiling using lowered Acoustic Doppler Current Profiler: Bottom track and inverse solutions. *J. Atmosph. Oceanic Technol.*, 19, 794-807, 2002.
- Picheral, M., Guidi, L., Stemmann, L., Karl, D. M., Iddaoud, G., &Gorsky, G. (2010). The Underwater Vision Profiler 5: An advanced instrument for high spatial resolution studies of particle size spectra and zooplankton. *Limnology and Oceanography: Methods*, 8(1), 462– 473. doi:10.4319/lom.2010.8.462.
- Guidi, L., Jackson, G. a., Stemmann, L., Miquel, J. C., Picheral, M., &Gorsky, G. (2008). Relationship between particle size distribution and flux in the mesopelagic zone. *Deep-Sea Research Part I-Oceanographic Research Papers*, 55(10), 1364–1374. doi:10.1016/j.dsr.2008.05.014.